1988

Excitation of surface plasmon polaritons on n-type GaAs for millimeter waves /

Dong-Hyun Hwang
Lehigh University

EXCITATION OF SURFACE PLASMON POLARITONS ON n-TYPE GaAs FOR MILLIMETER WAVES

by

Dong-Hyun Hwang

A Thesis

Presented to the Graduate Committee

of Lehigh University

in Candidacy for the Degree of

Master of Science

in

Electrical Engineering

Lehigh University

1988

This thesis is accepted and approved in partial fulfillment of the requirements for the degree of Master of Science.

5/11/68

Professor in Charge

Chairman of Department

Table of Content

List of Figures and Tables

Abstract

The excitation and detection of surface plasmons is achieved experimentally for an n-type GaAs substrate. Quasi-optical techniques are utilized to obtain the dispersion curve of these waves for the frequency range of 110 to 160 GHz. The experimental values are compared to the theoretical predictions. Both grating and prism coupling methods are discussed and implemented. Due to the dependency of the grating profile for periodic coupling structures, prism coupling data is mainly used to generate the final ω-β curve. Excellent agreement is found between the prism coupled data and theory.

I. Introduction

Due to a resurgence of interest in recent years for the millimeter and submillimeter region bands, there exists a need for development and operation of non-reciprocal devices at these frequencies. Ferrite materials have been used to design nonreciprocal components that function in the L through K bands and beyond. However, such materials experience substantial losses in the higher frequency ranges. As an alternative, theoretical considerations utilizing surface plasmons in a doped semiconductor as interface guided wave has shown reasonable losses for device purposes when operated at cryogenic temperatures [1]. Also, the feasibility of using properties of surface magnetoplasmons on semiconducting substrates for developing planar integrated non-reciprocal devices has been examined [2].

Experimental studies in surface plasmons are limited to works in the optical frequencies [3]-[6]. Even at these frequencies, very few reported obtaining experimental dispersion relations of surface plasmons on high mobility semiconductors [3]. In this paper, quasi-optical techniques for the generation of surface plasmon waves will be studied. Analysed are the prism and grated couplers as methods for excitation of surface waves and their possible application when used in conjunction with application of magnetic fields for non-reciprocal device application. Also, the dispersion relation for

a heavily doped n-type GaAs is obtained experimentally using prism couplers at room temperature. This data will be compared with the theoretical model. An unexpected mode is introduced for the experimental data. The additional mode will be interpreted and explained.

Overall excellent agreement between the theory and experiment was obtained for the frequency range of 110 to 160 GHz. The generation of surface plasmons for this frequency range has not been reported before, and plasmon generation on GaAs substrate has only been reported for optical frequencies [11]. This work will provide the first step in experimenting with materials capable of control of plasma density. The application of surface plasmons could provide a new array of millimeter wave devices with loss comparable to ferrite devices at lower frequencies.

II. Surface plasmons

2.1 Surface polaritons

As defined by Wallis ***et al.*** [7], a polariton is an electromagnetic wave coupled through phonon, plasmon, magnon or other type of excitation to condensed matter. In the literature, the term electromagnetic surface waves generally refer to guided modes propagating in a thin film on top of a metal substrate (see *fig. 2.1*). This type of surface wave is not a polariton and can be distinguished by examining its ω-β dispersion curve as shown in figure 2.2. In this paper, the phenomena of interest for guiding and controlling millimeter waves are surface plasmons, a member of the surface polariton family. This type of surface wave, for an isotropic n-type semiconductor, has the unique dispersion curve which lies entirely to the right of the light line in vacuum and is asymptotic to the surface plasma frequency (see *fig. 2.3*).

The theoretical dispersion of millimeter-wave surface plasmons in n-type GaAs was derived by Nurmikko ***et al.***[1], for an isotropic electron gas taking into consideration a simple Drude contribution to the dielectric constant.

$$\epsilon(\omega) = \epsilon^{(o)} - \frac{\omega_p{}^2}{\omega(\omega + i/\tau)} \quad = \quad \epsilon_s{}' + i\epsilon_s{}'' \qquad (2.1)$$

Where $\epsilon^{(o)}$ is the static dielectric constant of the material, ω_p is the plasma frequency

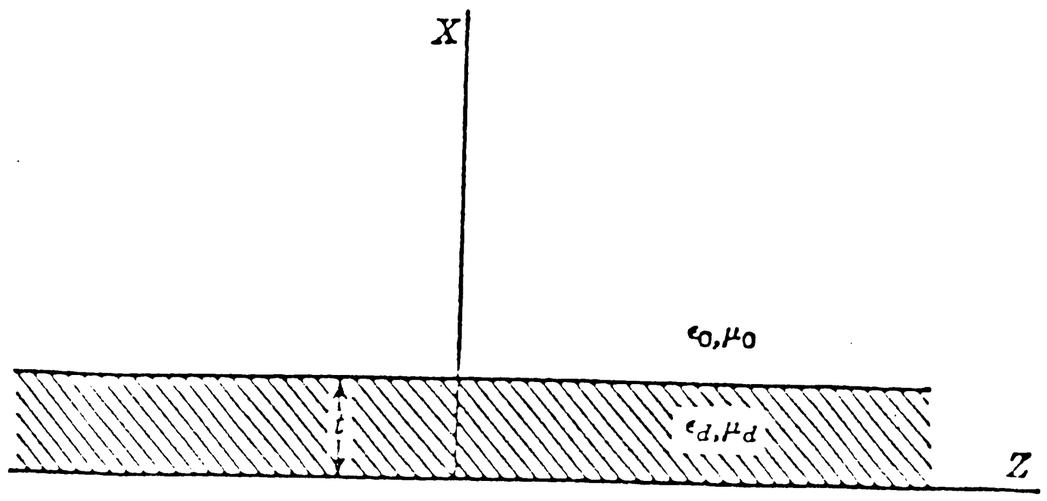

A dielectric-coated conductor.

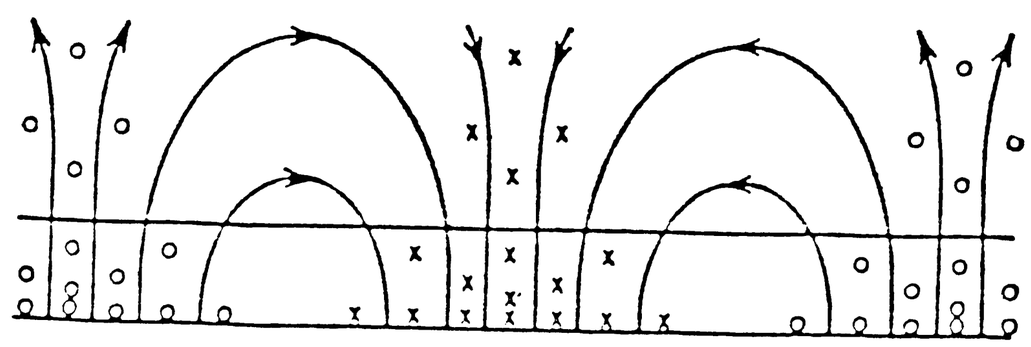

The TM_0 mode pattern for the coated conductor (ε lines solid.)

Figure 2.1 (from Harrington [9])

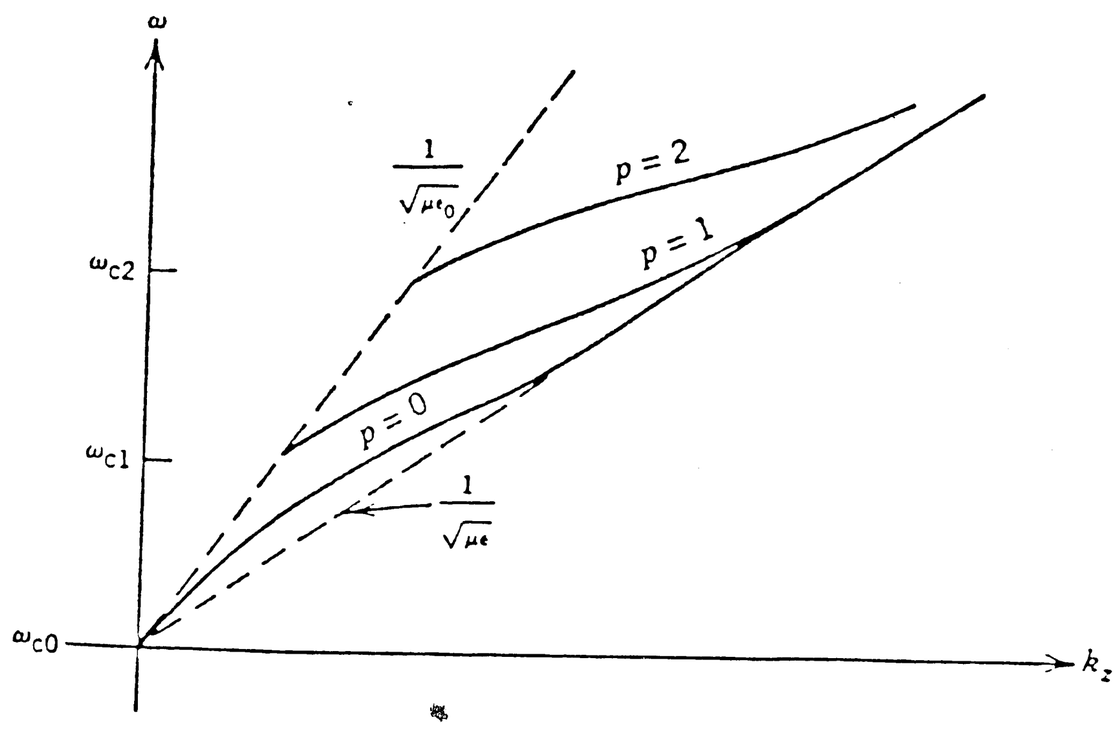

Dispersion relation for first three guided modes.

Figure 2.2 (from Lee [10])

$$\omega_s = \frac{\omega_p}{\sqrt{1+\epsilon^{-1}}}$$

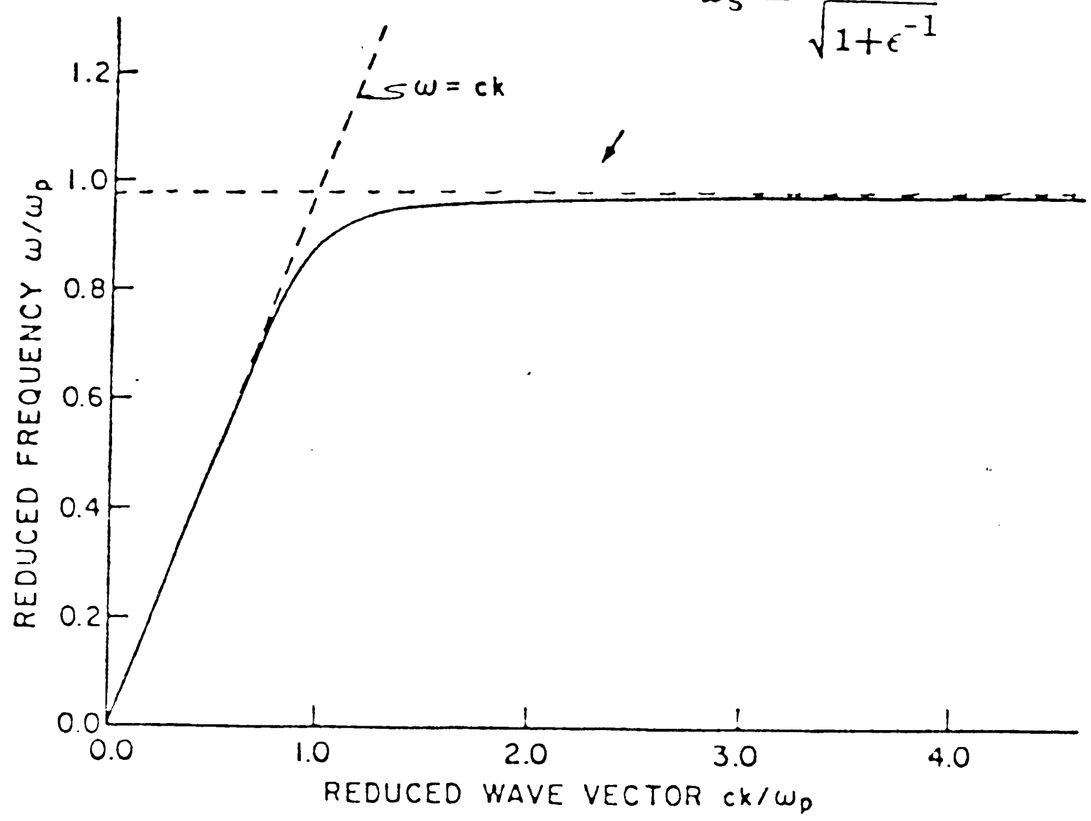

Dispersion curve for surface plasmon polaritons in n-type InSb.

Figure 2.3 (from Wallis *et al.* [7])

and τ is the momentum relaxation time. Equation (2.1) can be separated into real and imaginary parts so,

$$\epsilon(\omega) = \epsilon_s' + i\epsilon_s''$$

where
$$\epsilon_s' = \mathrm{Re}[\epsilon^{(o)}] - \frac{\omega_p{}^2}{\omega^2 + (1/\tau)^2} \tag{2.2}$$

and
$$\epsilon_s'' = \mathrm{Im}[\epsilon^{(o)}] - \frac{\omega_p{}^2}{\tau\omega(\omega^2 + (1/\tau)^2)} \quad .$$

Plotting $\mathrm{Re}[\epsilon(\omega)]$, we see it has large negative values at liquid nitrogen temperatures (77°K) with a carrier concentration equivalent to the plama frequency of $\omega_p = 10^{13}$rad/s for the frequency band of 110-170 GHz. For the same plasma frequency, but at room temperature (300°K), the real permittivity remains positive (see *fig. 2.4*). To obtain a surface plasmon wave, it is necessary for one of the media's effective permittivity to possess a sufficiently large negative real part. This requirement will be explained in the next section when the electromagnetic theory of surface polaritons is discussed. Since at room temperature the effective real permittivity is only slightly positive ($\simeq$ 3.0), adjustments in the carrier concentration and lowering of the temperature to increase mobility will lower the permittivity into the negative region. Although it is possible to obtain a desired range of values for the carrier concentration through plasma injection, it would be difficult to measure the exact carrier density.

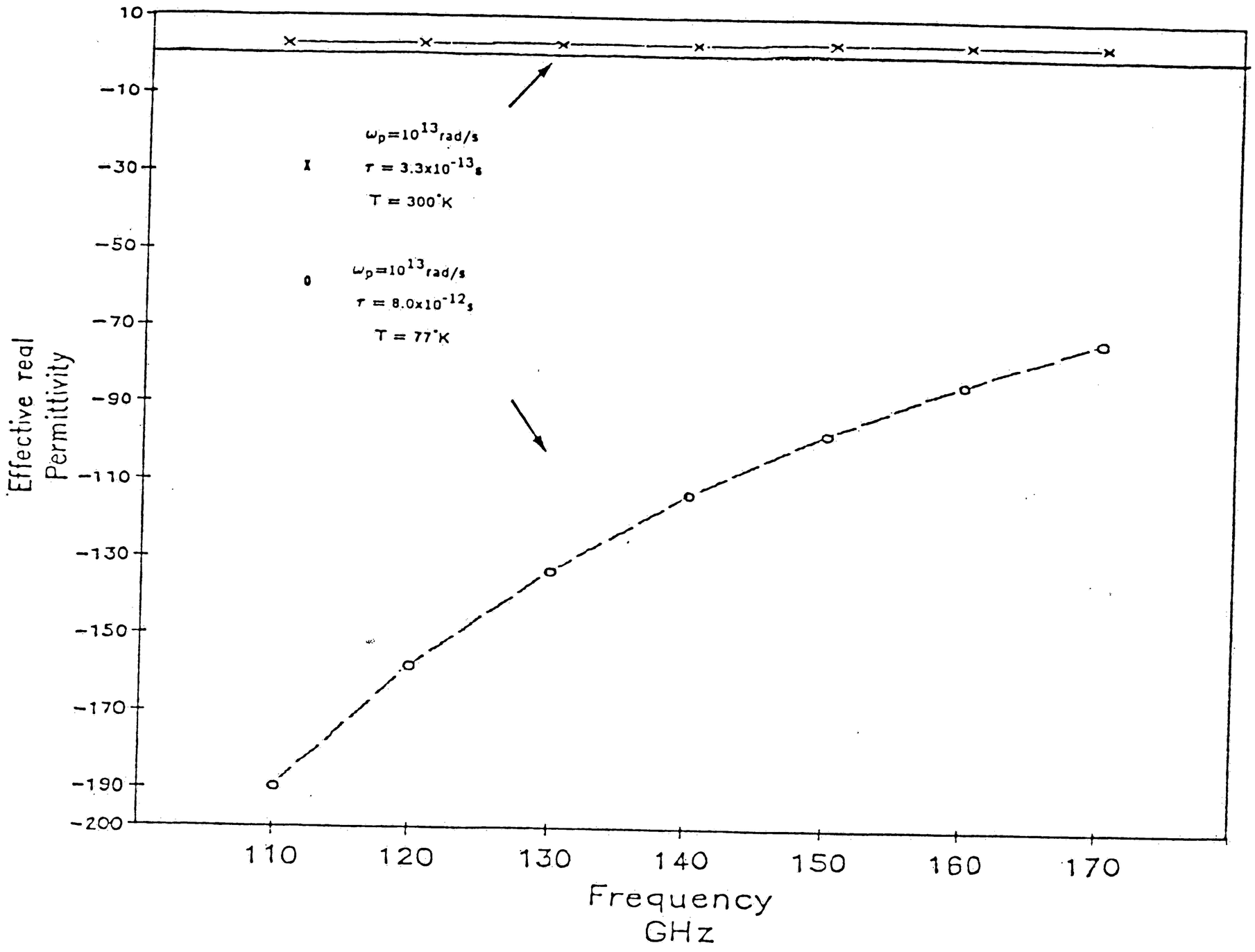

Figure 2.4 Effective real permittivity of n-type GaAs

contributed by this process. A problem also arises if optical injection methods are used. The depth of penetration for the newly formed plasma layer will be substantially less than the length of the millimeter wave, so the surface plasmon guiding structure becomes a three or even four medium layer, complicating the theory further. For our immediate purpose, a highly doped ($\simeq 1.0\text{x}10^{18}/\text{cm}^3$) substrate will be used to generate a lower portion of the dispersion curve without introducing concern over plasma injection problems.

2.2 Electromagnetic theory of surface polaritons

We consider a single planar interface of infinite extent which separates two media characterized by frequency-dependent dielectric constants $\epsilon_a(\omega)$ and $\epsilon_b(\omega)$ for $x > 0$ and $x < 0$, respectively. If the magnetic field is eliminated from Maxwell's curl equations, the electric field E satisfies the equation

$$\nabla\times\nabla\times \mathrm{E} + \frac{1}{\mathrm{c}^2}\frac{\partial^2 \mathrm{D}}{\partial t^2} = 0 \qquad (2.3)$$

We seek a solution to *eq.*(2.3) in which the electric field propagates in the z-direction and decreases exponentially with increasing distance from the interface. So, the equations for the electric fields in the two regions can be written as

$$\mathrm{E_a} = \mathrm{E_a}^{\mathrm{o}}\, \mathrm{e}^{-\alpha_a x}\, \mathrm{e}^{i(kz-\omega t)} \quad , \quad x > 0 \qquad (2.4)$$

$$E_b = E_b{}^o \, e^{\alpha_b x} \, e^{i(kz-\omega t)} \qquad , \qquad x < 0$$

substituting *eqs.*(2.4) into *eq.*(2.3), we obtain the decay constant for each region.

$$\alpha_a{}^2 = k^2 - \epsilon_a(\omega) \frac{\omega^2}{c^2}$$

(2.5)

$$\alpha_b{}^2 = k^2 - \epsilon_b(\omega) \frac{\omega^2}{c^2}$$

Applying the boundary conditions, at x=0 leads to the relations

(tangential) $$E_{ay}{}^o = E_{by}{}^o \quad , \quad E_{az}{}^o = E_{bz}{}^o \qquad (2.6)$$

(normal) $$\epsilon_a(\omega)/\epsilon_b(\omega) = -\alpha_a/\alpha_b \ . \qquad (2.7)$$

In addition, from the continuity of the tangential components of B, the following is obtained. $$(\alpha_a + \alpha_b) E_{ay}{}^o = 0 \qquad (2.8)$$

Since the decay constants α_a and α_b must be positive, $E_{ay}{}^o = 0$. Therefore for surface polaritons only TM mode propagation exists. Using *eqs.*(2.5) & (2.7), the well-known dispersion relation is obtained [1, 7, 8].

$$k^2 = \frac{\omega^2}{c^2} \frac{\epsilon_a(\omega)\epsilon_b(\omega)}{\epsilon_a(\omega) + \epsilon_b(\omega)} \qquad (2.9)$$

Equation (2.7) indicates that $\epsilon_a(\omega)$ and $\epsilon_b(\omega)$ must have opposite signs at the frequency ω. The medium with negative $\epsilon(\omega)$ is termed *surface active.* In the case of an air interface for ϵ_b, $\epsilon_a(\omega)<-1$. So this justifies the statement in section 2.1 regarding the requirement for a media to have an effective real permittivity of negative value.

2.3 Theory for highly doped GaAs

For a doping level in the order of $10^{18}/cm^3$, GaAs exhibits an effective dielectric constant with large negative values for the real part of the permittivity in the near millimeter wave range of 110 to 170 GHz. To obtain the effective permittivity, we have to calculate the plasma frequency and the relaxation time from the carrier concentration. The plasma frequency is defined by

$$\omega_p{}^2 = \frac{ne^2}{\epsilon_o m^*} \qquad (2.10)$$

where n is the carrier concentration of the material. Since for the doping level of 10^{18}, the plasma frequency ω_p is about $2.18x10^{14}$ rad/sec, the operating bandwidth is well below the asymptotic value of the surface plasma frequency ω_{sp}. The relaxation time τ, can be deduced from the DC conductivity $\sigma(0)$, if τ is assumed to be frequency independent. Since the frequency-dependent conductivity is defined by

$$\sigma(\omega) = \frac{ne^2\tau}{m^*} \frac{1}{1\text{-}i\omega\tau} \qquad (2.11)$$

and we obtain the DC conductivity by setting ω=0, $\sigma(0)= ne^2\tau/m^*$. M/A-Com, the manufacturer of the GaAs wafers, indicated an overall edge and center resistivity of $2.6x10^{-3}\Omega$-cm for the Si-doped samples. From the resistivity, an impurity concentration of $8x10^{17}/cm^3$ can be deduced from the curve in Sze [21] for room temperature (T=300°K) n-type GaAs. This value is very close to the carrier concentration of $10^{18}/cm^3$ indicated by the manufacturer, so we can reasonably

assume all the impurities are ionized at room temperature. With $n=1.0x10^{18}/cm^3$ and $\sigma(0) = 384.6\ /\Omega\text{-cm}$, a value of $\tau = 9.169x10^{-14}$sec is obtained. The corresponding change in the real part of the permittivity ϵ_s' in eq.(2.2) can be calculated as a function of ω for the obtained ω_p and τ. Since $1/\tau$ is large compared to the operating ω range, the $\Delta\epsilon_s'$ is almost a constant at about -385. This yields an effective real permittivity of $\epsilon_s' \simeq -382$ if $Re[\epsilon^{(o)}]$ is assumed to be 13.0. The change in the imaginary permittivity is $\Delta\epsilon_s'' \simeq -4{,}030$. If $Im[\epsilon^{(o)}] = 1{,}000$ is assumed, the complex effective permittivity for the frequency range of 110-170GHz is about $\epsilon_s \simeq -382 - i3{,}030$. Using this constant effective permittivity, the dispersion relation is simplified.

The dispersion relation for surface plasmons is given by Ward *et al.* [16] where the propagation constant for an air interface is given by

$$\beta = \frac{\omega}{c}\sqrt{\frac{(A+\sqrt{A^2+B^2})}{2D}} \qquad (2.12)$$

where

$$A = |\epsilon|^2 + \epsilon'$$

$$B = |\epsilon|^2 + \epsilon'' \qquad (2.13)$$

$$D = |\epsilon + 1.0|^2$$

and $\epsilon=\epsilon'+\epsilon''$ is the effective dielectric constant of GaAs. The theoretical dispersion curve for a sample with a carrier concentration of $1.0x10^{18}/cm^3$ is a constant line slightly to the right of the light line for the frequency range of 110 to 170 GHz. In the

case of n = $1.0\text{x}10^{18}/\text{cm}^3$, $\omega_p = 2.18\text{x}10^{14}$ rad/sec and for $\tau = 9.17\text{x}10^{-14}$ sec, the propagation constant has the relation , $\beta = (\omega/c)\ 1.098$. If a simple model is used without taking the Drude model into consideration, the dispersion relation is not altered by a great amount, since $\beta \simeq (\omega/c)\ 1.026$.

III. *Excitation of the surface waves, theory :*

Nonradiative modes can only be excited at wave vectors k larger than the photon wave vector ω/c. The first of two common methods of obtaining larger k vectors is utilizing the attenuated total reflection (ATR) technique of the prism coupler. This technique is limited to a range of values obtainable by the prism coupler itself. The second method is to use a periodic structure on the surface which couples to the incoming photon. The theory for grated couplers will be described first.

3.1 Grating coupler theory

In grating couplers, the surface wave must be accompanied by space harmonics in the grating region because of the periodic nature of the structure. These harmonics have propagation constants given by

$$\beta_m = \beta_o + \frac{2m\pi}{d} \qquad m = 0,\ \pm 1,\ \pm 2,\ .... \qquad (3.1)$$

where β_o is closely equal to the surface wave propagation constant if the periodic structures are considered to be small perturbation and d the periodic spacing. The phase matching condition can be satisfied if

$$k \sin\theta = \beta_m \qquad (3.2)$$

where θ is the incident beam angle to the periodic structures.

Experiments with grating couplers on semiconductors such as GaAs [11] and InSb [3] were conducted earlier. The construction of a dispersion curve $\omega(\beta)$, involves the determination of eigenfrequencies ω_r, which depends on the grating profiles. Experimentalists have encountered the well known Wood's anomalies for gratings. This is illustrated in figure 3.1. Theory and experiment have shown that the modulation depth h of the periodic structures contributes significantly to the shape of the disperion curve [12,13]. Since the experiment is performed using high index line strips of rectangular shape polymer material as the periodic corrugation, better coupling is expected than for grooves drawn on the substrate surface. The only difference in theory between grooves and high index structures is a refractive index term n_p, multiplied for the material used as grating structures on the left-hand side of eq. (3.2). So $\beta_m = n_p k \sin\theta$ and $n_p \simeq 1.60$ for polymer dielectrics at the operating frequency range of 110 to 170 GHz. The maximum achievable efficiency of coupling for such periodic structures is 80.1% [14]. This condition is obtained for the optimum αw_o

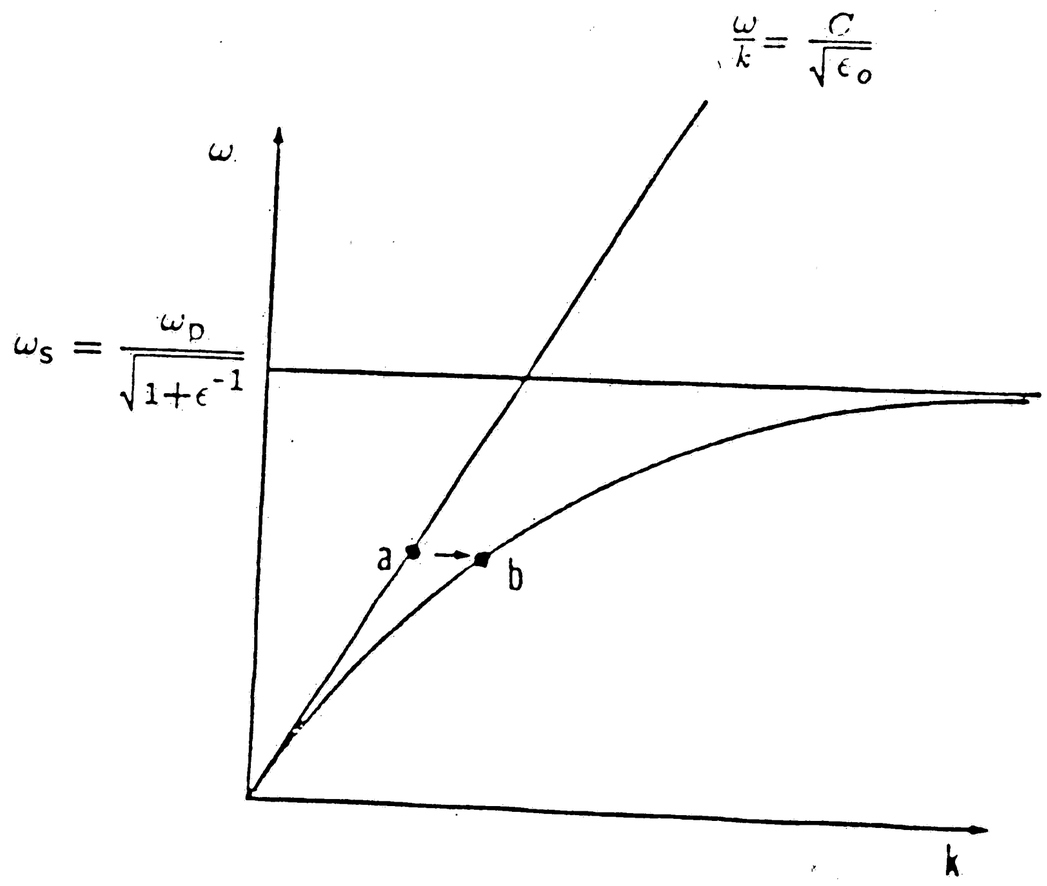

Figure 3.1 Description of Wood's anomalies

value of 0.68, where

$$w_o = w \sec\theta \tag{3.3}$$

w is the half beam-width of a Gaussian beam and α is the leakage factor. The leakage factor depends very much on the height of the grating [15]. If the length of the period d, is half of the wavelength, and h, the height is about $0.1mm$ at λ=$2.0mm$, the leakage factor is approximately $3.75/m$. The constraint on the beam width for this range of wavelength is

$$0 < w < 18.1\ cm \qquad \text{for} \quad 0 < \theta < \frac{\pi}{2}$$

so for practical high efficiency coupling at $0.1mm$ of grating height, about 1° to 5° of incidence angle will be optimal to obtain a reasonable beam width from a waveguide horn. Since we are involved in experimenting at considerably shorter wavelength than is the case for microwaves, most of the theory is obtained from optics. However, various experiments will have to be conducted to obtain a reasonable interpretation for the quasi-optical theory applied to the millimeter wave range.

3.2 Prism coupler theory

The use of attenuated total reflection (ATR) method for wave excitation has been a common technique in waveguided optics [17,18]. More common terminologies

used are the prism coupling or optical tunneling techniques. The surface plasmon excitation technique was first suggested by Otto [19] and followed by a modified technique by Kretschmann [20] for thin samples. The theories behind this method of surface plasmon excitation are basically identical to that of guided optics. In guided optics, the dielectric layer is bounded by a top and bottom layer and the incident wave travels along a zig-zag path exhibiting total reflection at both layers. The wave in surface plasmon is bounded on top by an active surface and a below extends to infinity. Both configurations have to match the propagation constant at the base of the prism to the guided wave mode or the surface plasmon propagation constant. In the guided wave case, the theory becomes more complicated as consideration of various allowable modes for the dielectric thickness limits the material selection for the prism coupler. This restriction is more evident in semiconductor guides where the refractive indexes range from 3.0 to 4.0. Since, to excite a guided mode, the prism coupler's refractive index has to exceed the guide's effective refractive index, optical range wave guiding had to be achieved through end coupling. The use of millimeter waves provide new flexibilities in selecting prism couplers for semiconductor guides. This is due to the reduced effective refractive index contributed by the carriers.

The Otto or guided wave configuration has a gap between the prism and the guide. This gap is usually of the order of the wavelength and it is usually considered to

be air, although index matching dielectrics can be used to fill the gap. The Otto configuration works through a phenomenon referred to as frustrated total internal reflection. The ATR technique utilizes the evanescent tail formed through the prism to couple to the surface wave (both surface plasmon and guided wave). Since surface waves are non-radiative, the propagation constant required is to the right of the light line in the ω-β diagram. This can be achieved by forming an incident wave above the critical angle of the prism-gap interface. When the incident wave is totally reflected the reflected intensity shows a dip at the resonant coupling condition. This loss in energy corresponds to the energy conversion into the surface wave. The dispersion relation, for a resonant angle of incidence θ_i, can be expressed by $\beta(\omega)=\omega/c\ n_p \sin\theta_i$.

IV. Experiment and results

4.1 Experiment setup

The source of the millimeter wave was a Micro-Now model 705B millimeter wave sweeper with a model 170 BWO tube. The output power averaged about 10mW for the frequency band of 110 to 170 GHz. Our measurements were performed using a bolometer. A signal generator was used to modulate the tube at 1kHz. The

modulation was triggered by a TTL signal and was connected to the amplitude modulation input (AM). The TTL signal was also connected to the reference input of a phase locked amplifier (EG&G Princeton Applied Research model 5207). The modulated millimeter wave output was connected to a Hughes model 45728H-1000 attenuator with a range of 0 to 50dB of attenuation and a maximum insertion loss of 2dB. A directional coupler was followed by the attenuator. The Hughes coupler model 45328H-1210 is a 3 port split block style general purpose coupler with a low frequency band crossguide coupling value of 10dB. The second line output from the coupler was connected to the leveler input of the generator. The main line was connected to a waveguide horn. The pyramidal horn has a 24dB gain at mid band. The reflected and surface transmitted signals were detected by a flat broadband detector connected to a receiver waveguide horn. The detector has a minimum sensitivity of 100mV/mW. Signal detection was achieved by using the phase lock-in amplifier. The general schematic of the setup is shown in figure 4.1.

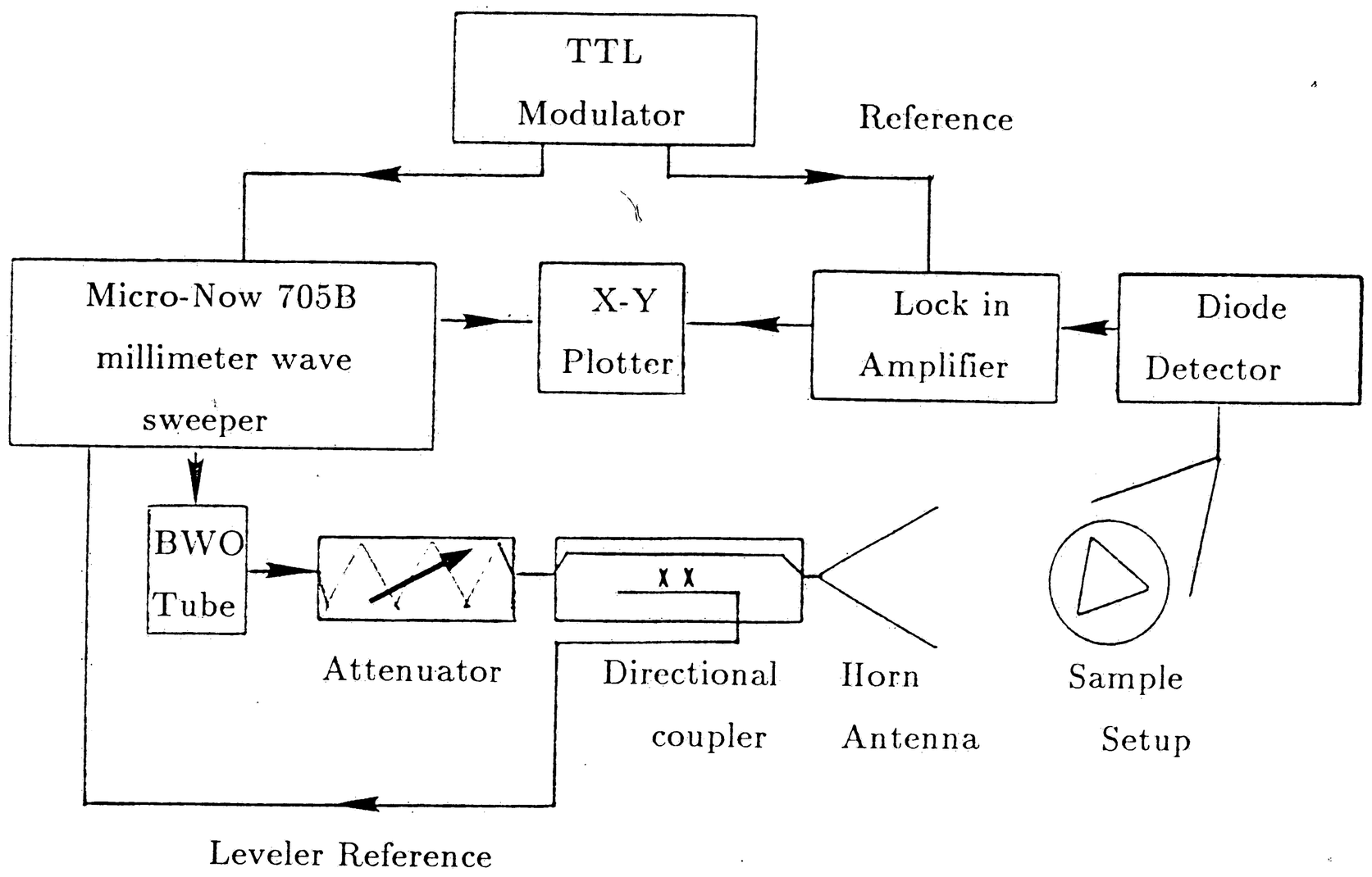

Figure 4.1 Block diagram of experimental setup

4.2 Periodic grating experiment

In this experiment, the M/A-Com GaAs sample was placed at 45° and reflective intensity measurements between the polished sample and the sample with periodic lines of 2mm were compared (see figure 4.2). The lines were 2mm wide, 0.1mm thick and composed of cellophane. The millimeter wave sweeper was swept from 140 to 170 GHz. Initial comparison showed a dip at about 163.6 GHz in the reflected intensity for the sample with the periodic structure (see figure 4.3). To check for surface wave coupling, the receiver was placed at the edge of the sample to obtain signal detection. The receiver detected two signals with strong intensities at 146.3 and 163.6 GHz (see figure 4.4). The experiment was repeated with power leveling and with a directional coupler and we obtained a sweep of a narrower bandwidth (158 to 164 GHz). The results, as depicted in figure 4.5, show a drop in intensity at 163.6GHz for the grated sample as compared to the polished sample. Also, there is strong detection of a signal at the edge of the sample at the same frequency. Another experiment with d=1.5mm was conducted at 23°. Since the periodic length was not in the $\lambda/2$ regime, very weak coupling was observed for this case. The results are evident in figures 4.6-7. The reflection drop at 160.7 GHz is not as well defined as in the previous case and the end signal detection is disturbed by noise levels as strong as the signal itself. Another

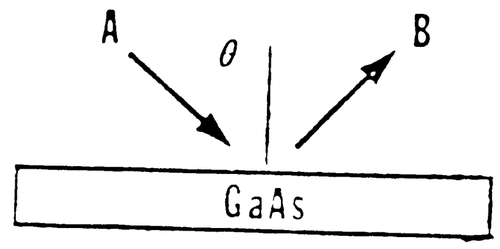

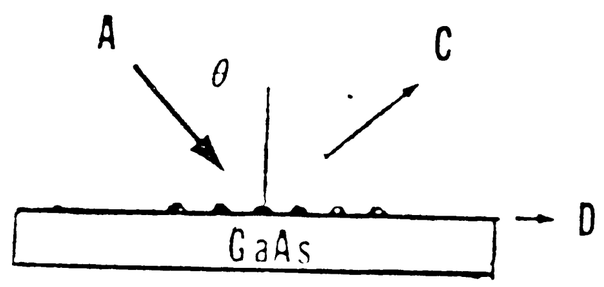

Figure 4.2 Sample comparison experiment

A - Incident beam from source

B - Reflected beam from polised sample

C - Reflected beam from sample with periodic structures

D - Surface wave beam

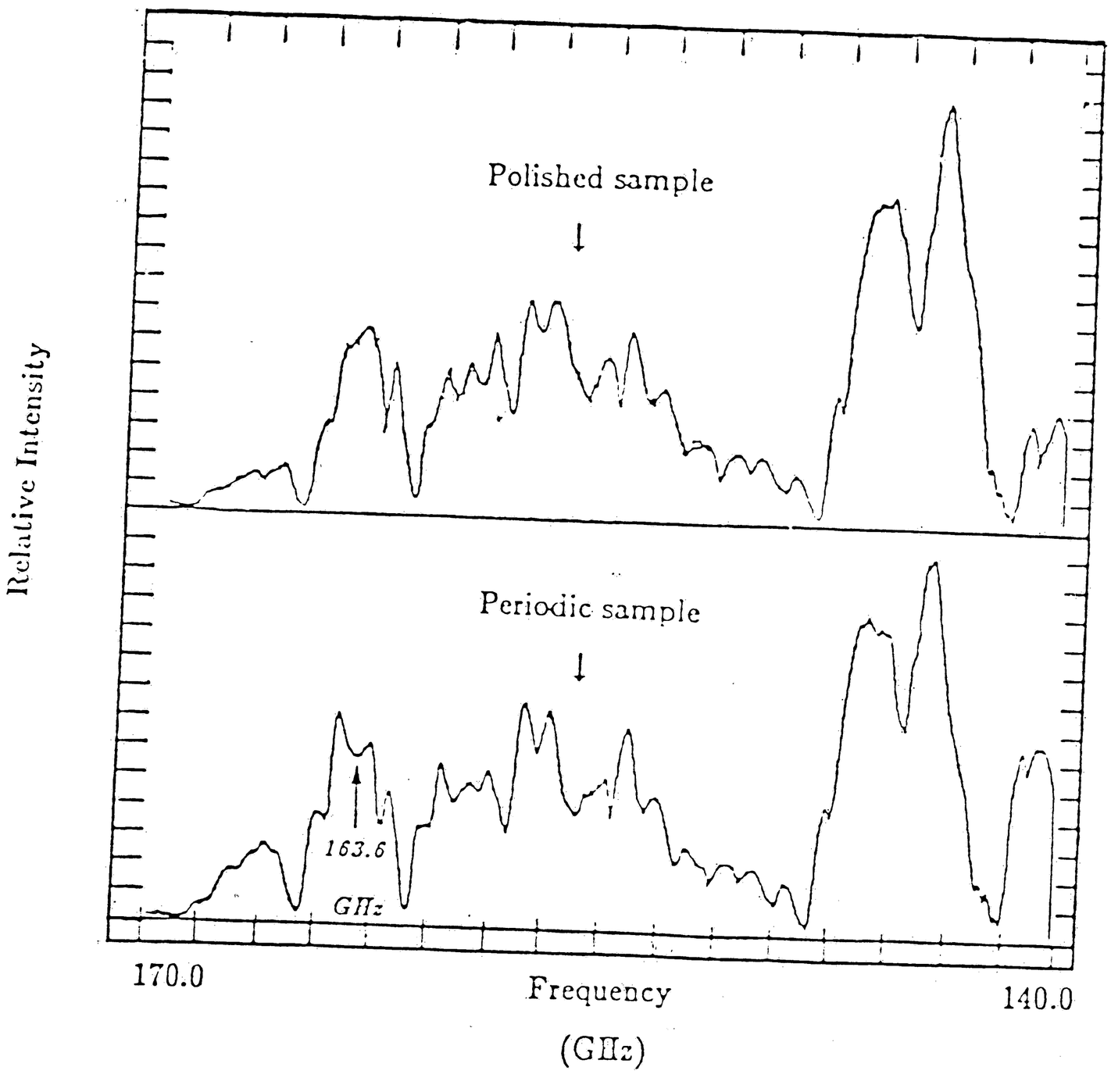

Figure 4.3 Comparison of intensity of reflected beams

(For $\theta = 45^{\circ}$ and $d = 2$ mm)

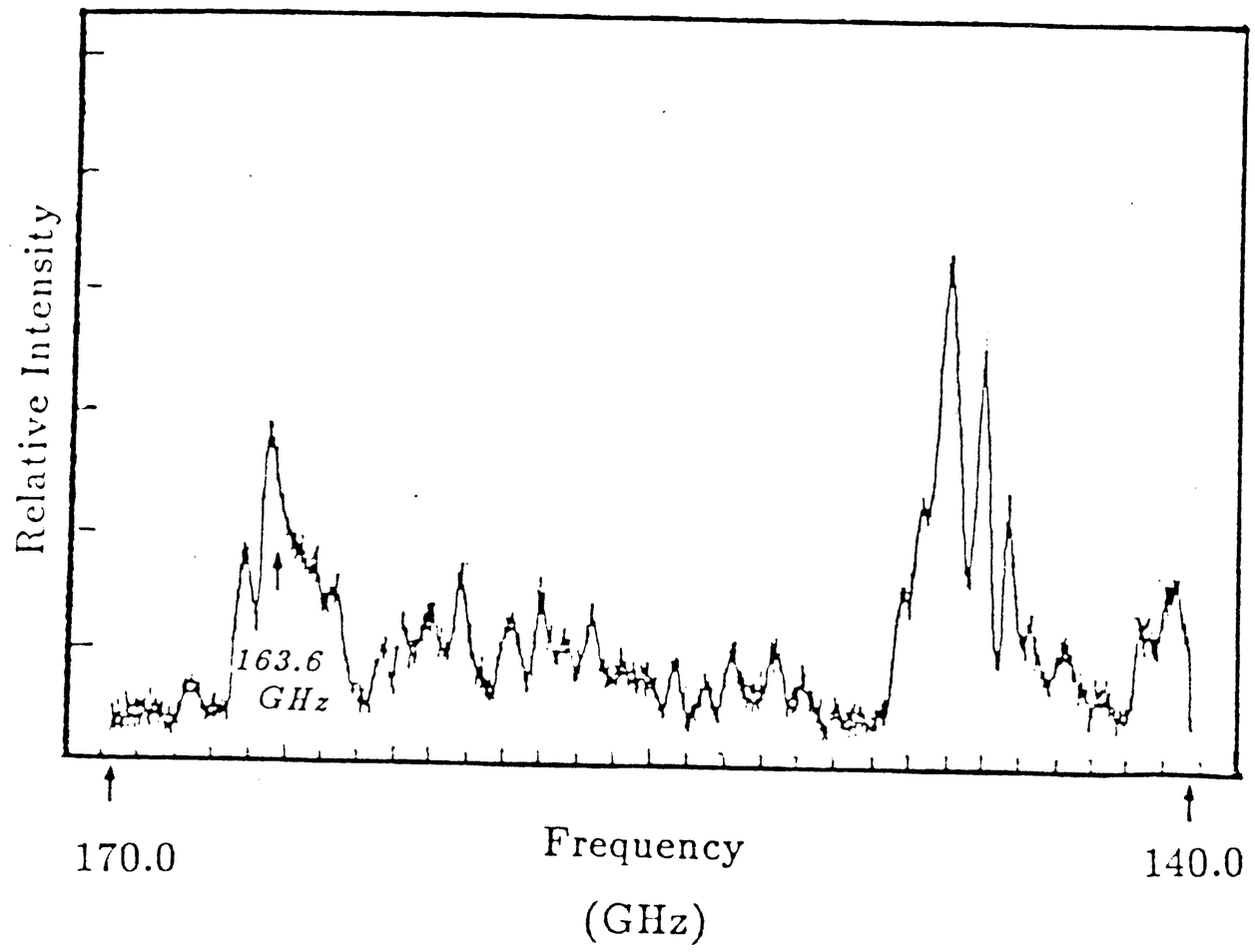

Figure 4.4 End detection for coupled wave

(For θ=45° and d=2mm)

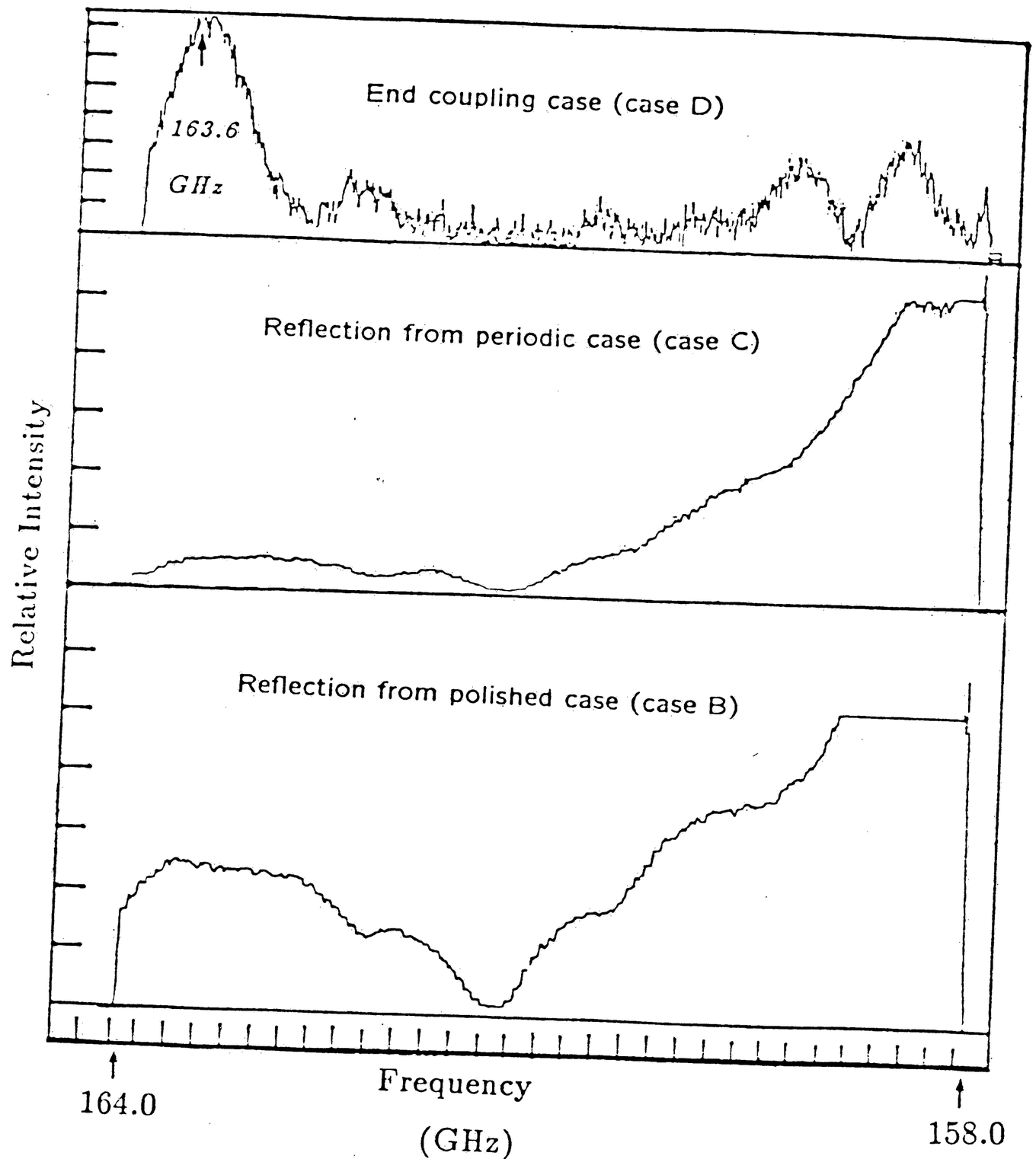

Figure 4.5 Sweep at a narrower bandwidth

(*For* $\theta = 45^{\circ}$ *and* $d = 2mm$)

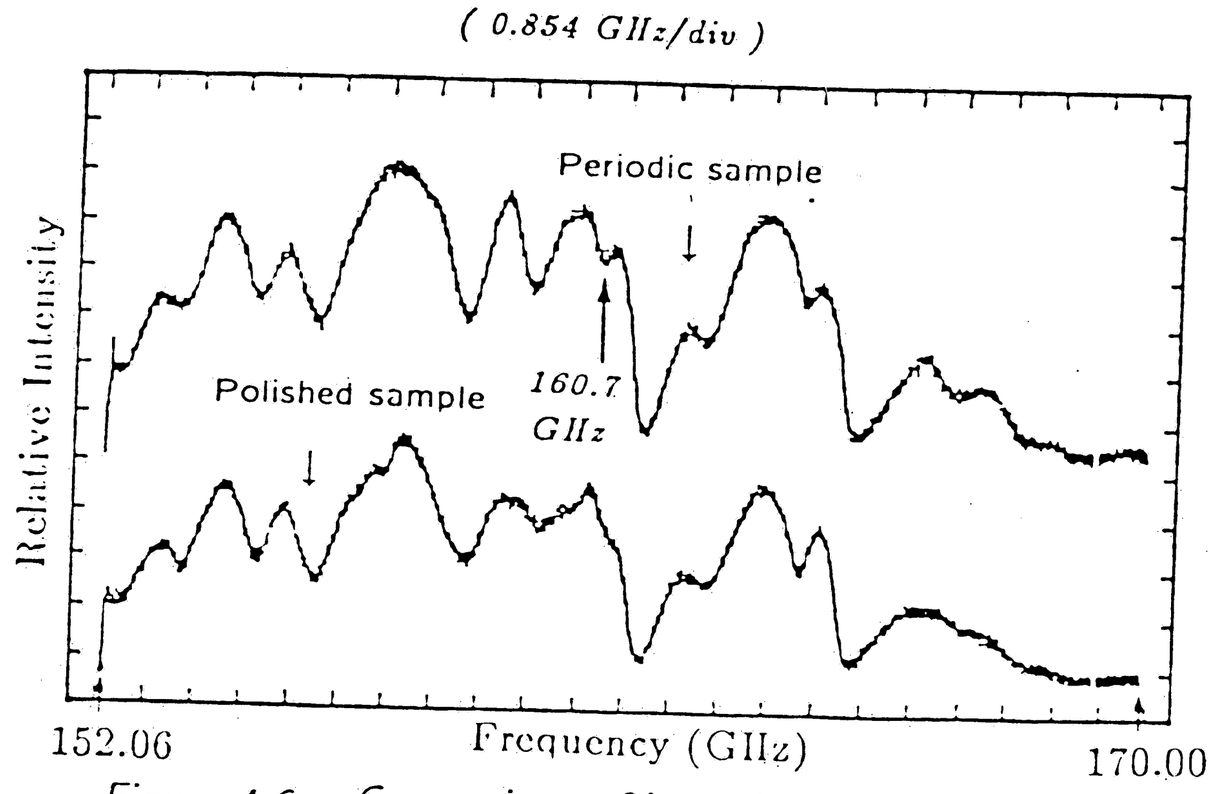

Figure 4.6 Comparison of intensity of reflected beams

(For $\theta = 23^{\circ}$ and d=1.5mm)

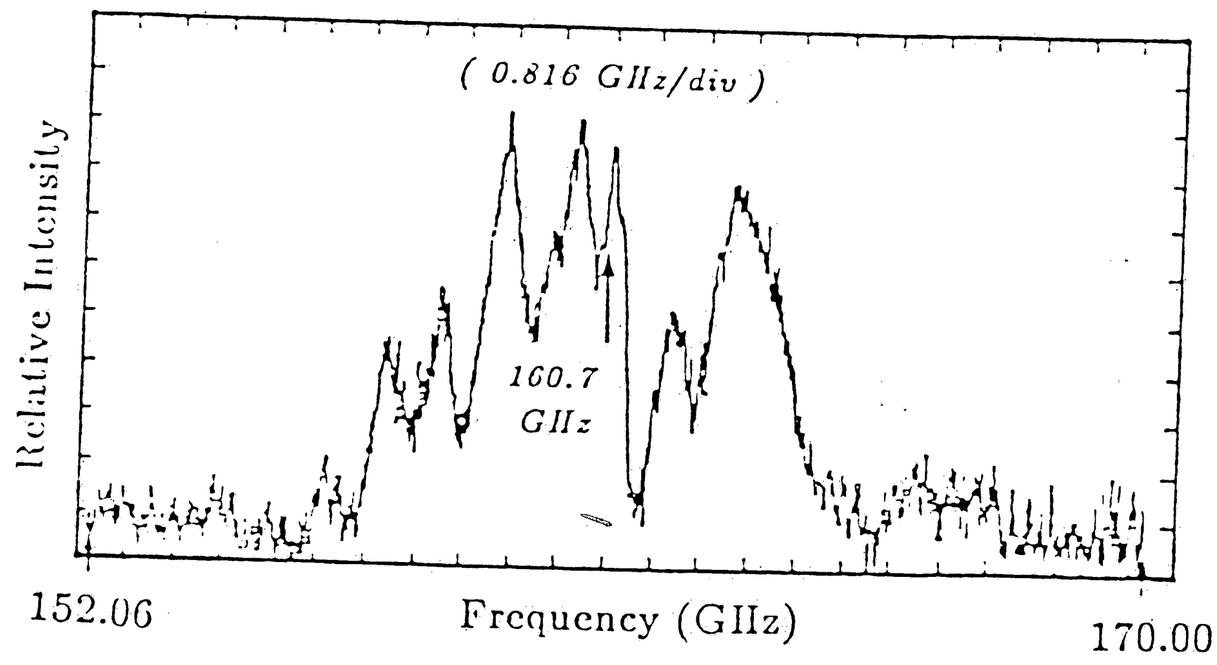

Figure 4.7 End coupling intensity of sample with periodic structures

(For $\theta = 23^{\circ}$ and d=1.5mm)

experiment was carried out with the enhanced gratings being three times greater in height than in the previous case. The sweep frequency was narrowed to a range of 158.4 to 164.5 GHz. The results are depicted in figure 4.8 which shows an increase in the number of end coupling peaks. In this case, the detection of the particular coupling frequency is hampered by an increased number of harmonics or noise. This particular experiment shows that a complicated diffraction and reflection theory would have to be taken into account. Although a few very involved theories are published, to pursue these would be too much of a distraction from our immediate desire of observing surface plasmon waves. Although there is strong evidence of surface plasmon generation at 2mm of grating distance, the height and shape of the particular grating structure influences to a high degree the detection procedure for the surface wave. A more practical and nondestructive method is the prism coupling configuration which will be discussed in the next section. The grating coupler dips obtained will be compared with the prism coupled surface wave in the ω-β diagram. The reason for this is to eliminate any doubts in the our grating data as to it being of higher or lower harmonic origin. A comparison will illustrate the more accurate method of surface wave generation for a particular frequency range. The final reasoning for not utilizing the periodic sturcture method is the presence of the scattered of waves which contribute to a high level of noise.

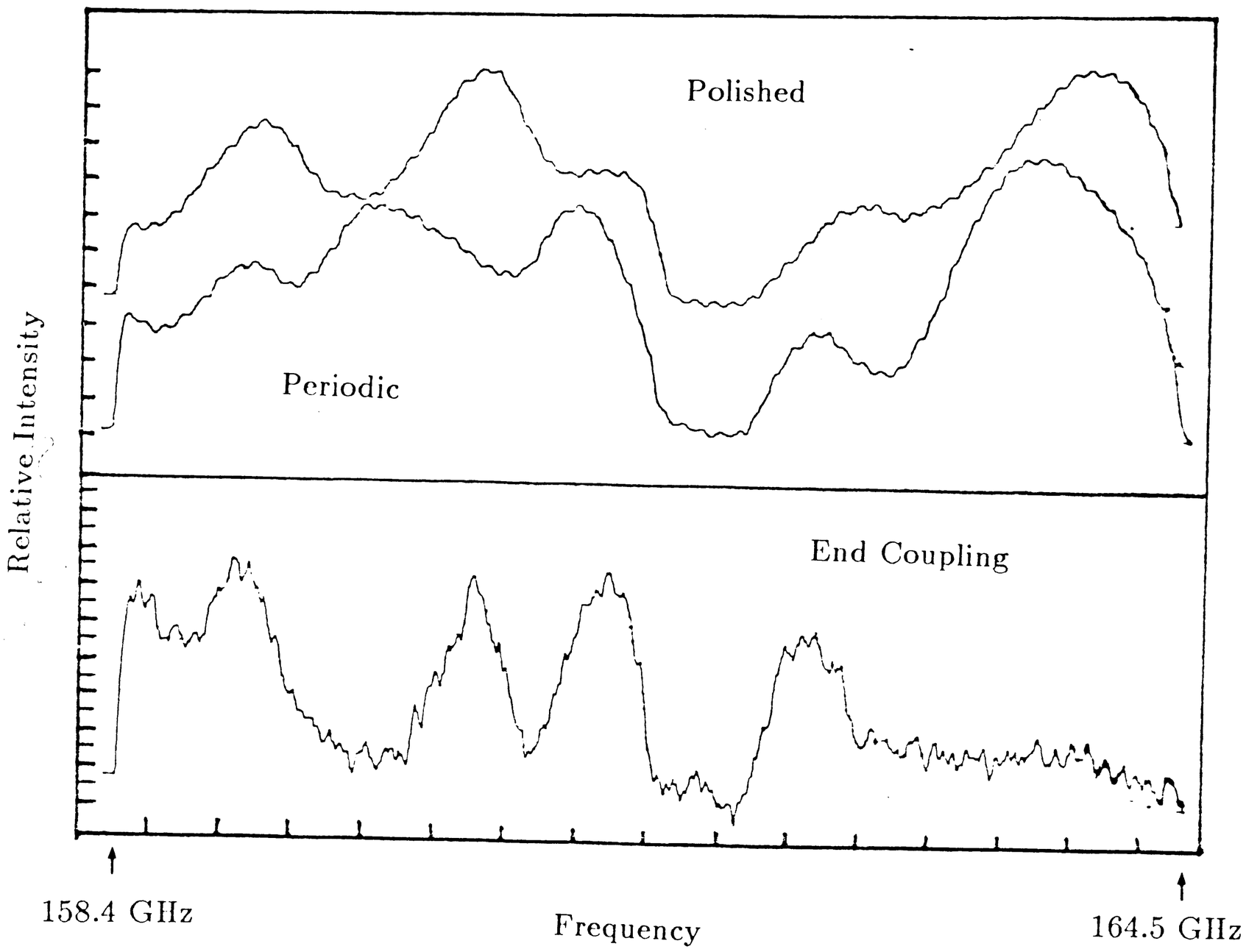

Figure 4.8 Higher grating profile coupling intensity (158.4-164.5 GHz)
(θ=23° , d=1.5mm)

4.3 Prism Coupling experiment

In comparison to grating couplers, prisms provide a non-destructive way of generating surface plasmons. It also eliminates the need to worry about the complicated scattering theories needed for grating profiles. So, Wood's anomalies should not be encountered as in the previous experiments conducted using enhanced periodic structures. The method used in this experiment is shown in figure 4.9. The setup is referred to as the Kretschmann configuration [20]. This configuration differs from the traditional Otto configuration because the gap between the prism and the metal is eliminated. To use this method, the thickness of the surface active material has to be restricted to less than the order of the operating wavelength (usually $\lambda/10$). Since the wafer of the GaAs is 25mils or 0.0635cm, the operation in the frequency range of 110 to 170 GHz results in a surface active thickness of order $\lambda/4$.

When performing this experiment, the prism was separated by a distance of 16cm from the source horn. This was to ensure far zone operation and plane wave incidence could be assumed ($2D^2/\lambda$). Experiments were conducted for reflection angles of 37°, 45°, 51°, and 57° at the prism base. Millimeter wave sweeps were performed for two bandwidths of 110 to 136 GHz and 136 to 159 GHz. Distinctive sweeps at four differing angles of incidence were performed. The experiments were conducted both with and without the GaAs. The data is shown in figures 4.10 to 4.13. and the

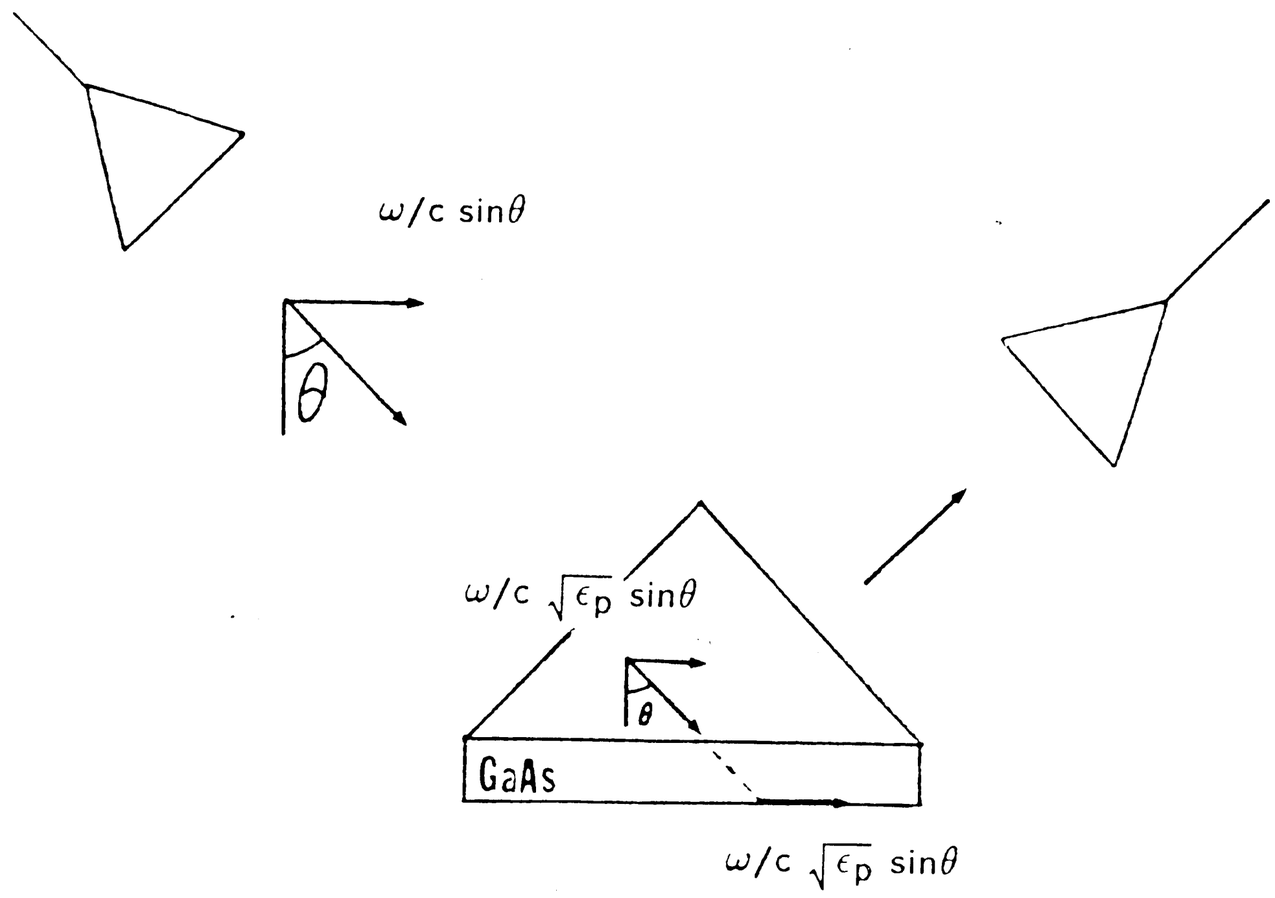

Figure 4.9 The Kretschmann configuration

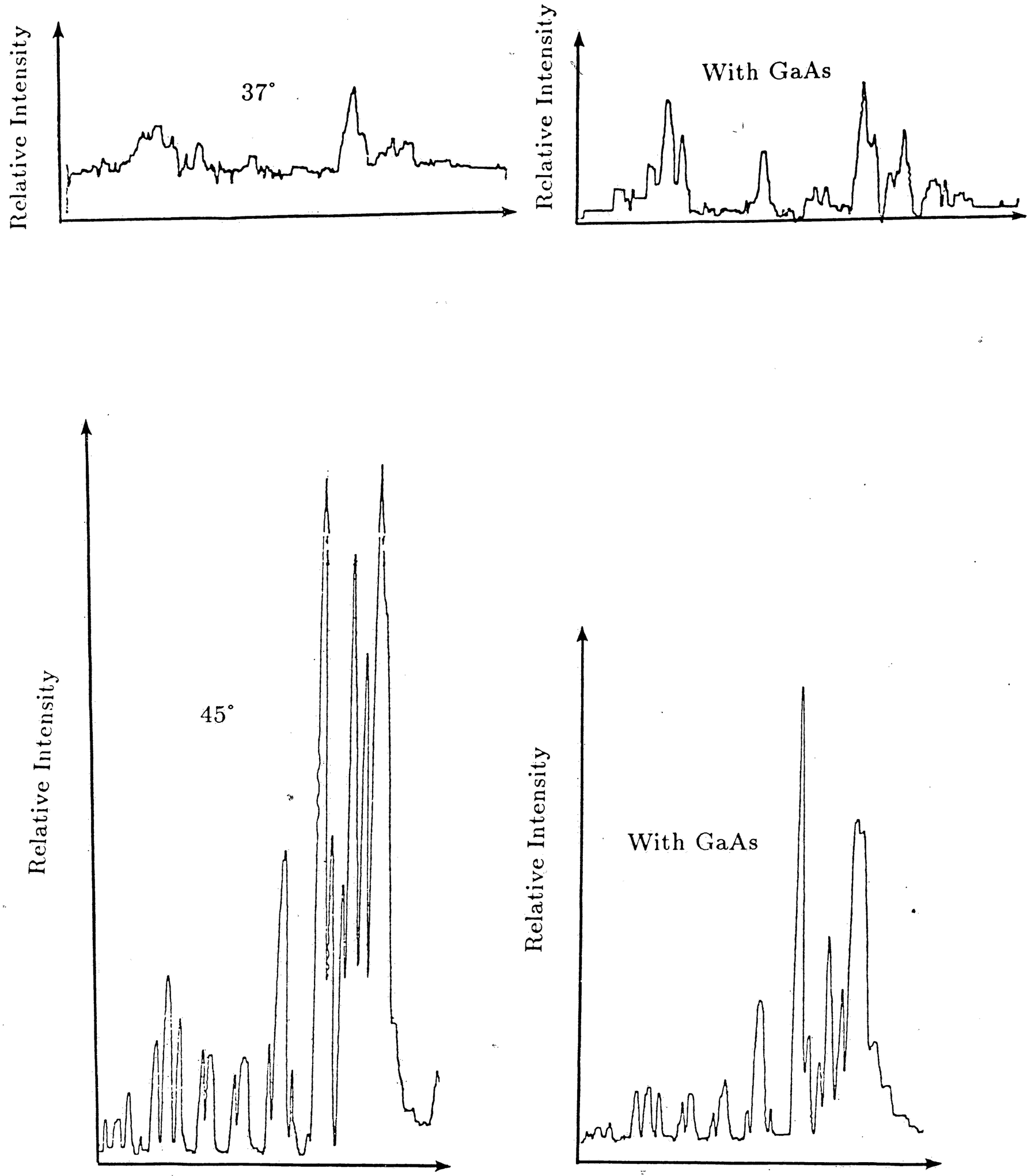

Figure 4.10 Prism coupler intensity comparison (110-136 GHz)

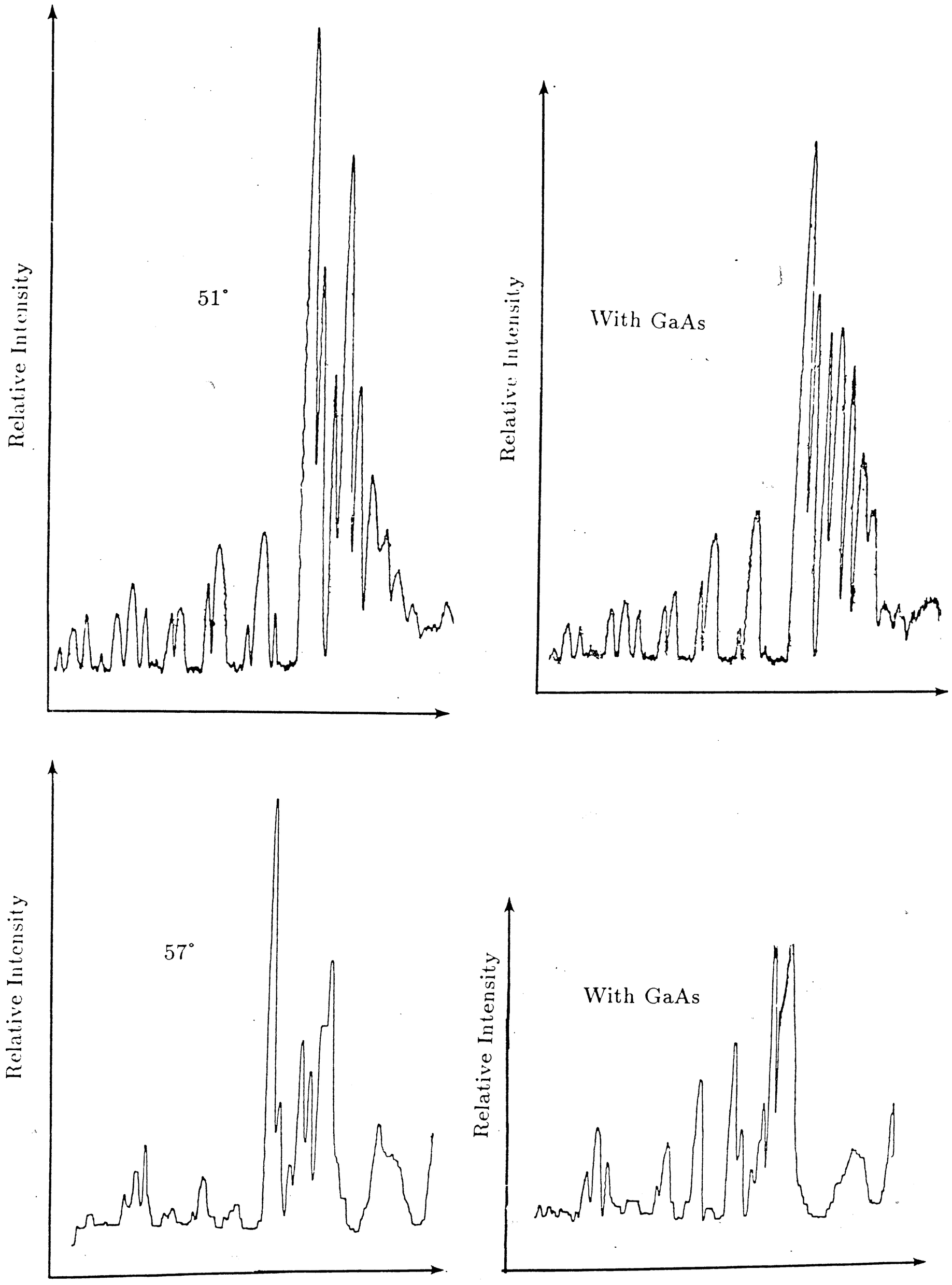

Figure 4.11 Prism coupler intensity comparison (110-136 GHz)

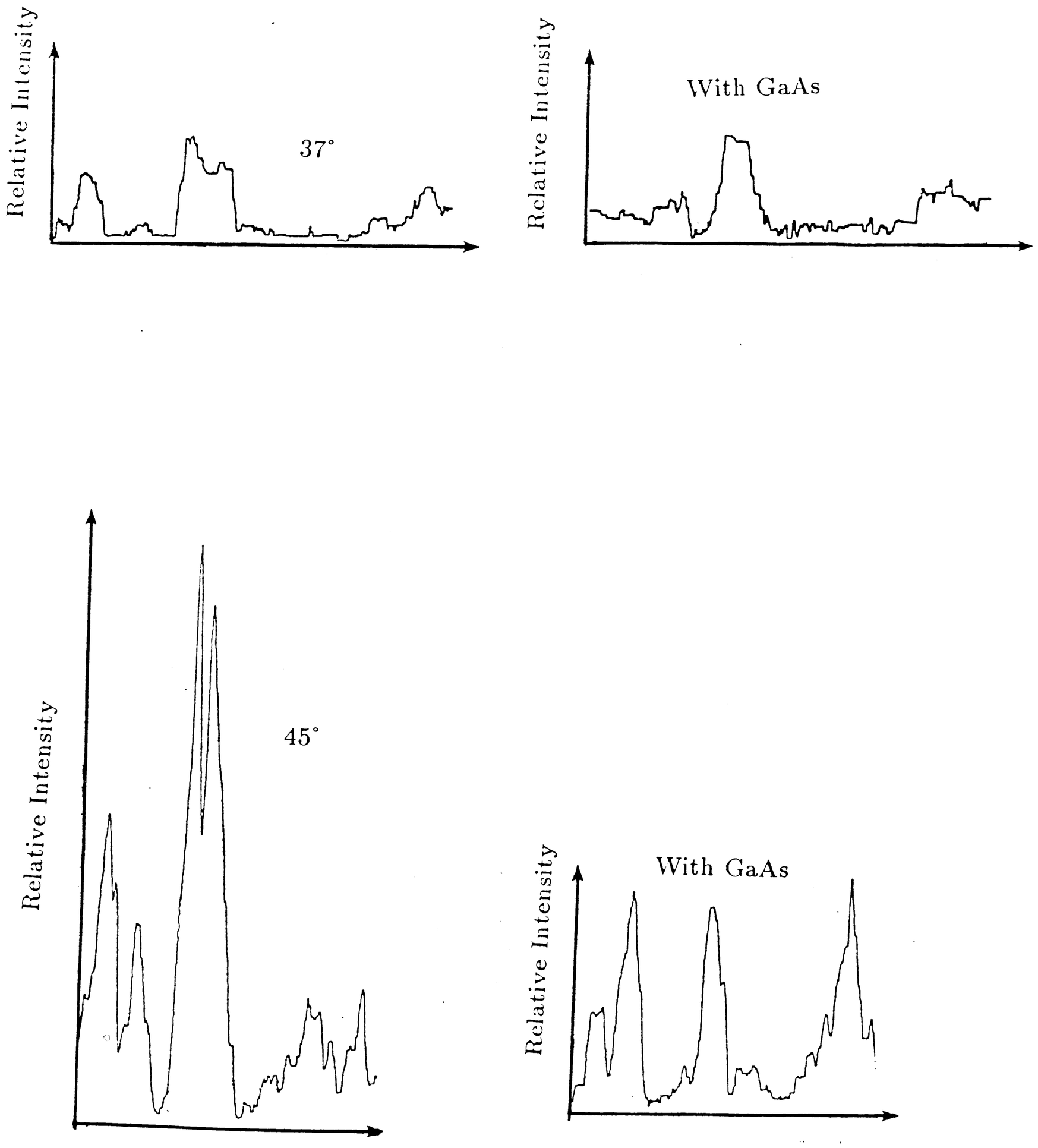

Figure 4.12 Prism coupler intensity comparison (136-157 GIIz)

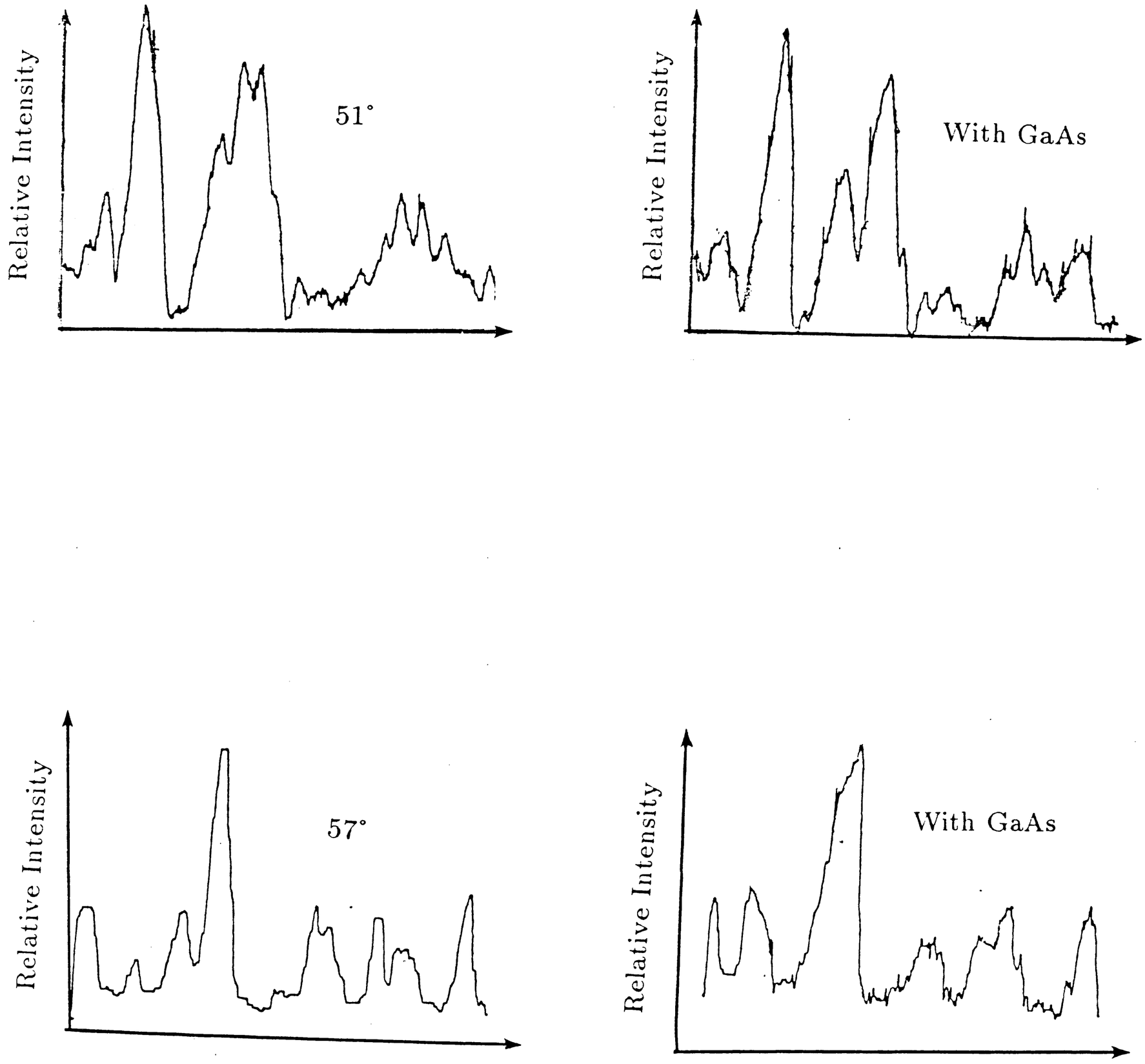

Figure 4.13 Prism coupler intensity comparison (136-157 GIIz)

the resulting sweep was normalized to obtain the plane polarized reflection coefficient for each case. As observed in figures 4.14 to 4.17, various minimums are to be observed for the two bandwidths of 110-136 GHz and 136-159 GHz. Careful consideration of these minimum points is required to interpret the data correctly. First, the obtained minimums are used to calculate the propagation constant β, which will help determine the correct minimums when plotted against the normalized plane polarized reflection coefficient. The obtained minimas were labeled and normalized to obtain the frequency of the minimum for each angle of incidence. Theoretically, the surface plasmon wave is generated when the reflection coefficient approaches zero. In the experiment performed, the minimum normalized value obtained was about 0.05 or -13.0 dB. As variation in the incident angle is introduced, the reflection coefficient changes. The desired angle of observation is that which yields the minimum reflection at a given frequency. For this experiment the accuracy of the angle of incidence is limited to about $\pm 2^{\circ}$ and if a more accurate method of angular measurement was available, near zero levels of normalized minimum should be observed. Some mimiums will be closely matched to the incidence angle and most points will be in the vicinity of this angle. Interpolation of angles is necessary to yield the full continuous ω-β curve.

In table 4.1, the points *A* through *M* showed the most clearly distinguished minima when plotted against the propagation constant. The minimum usually ocurrs for the

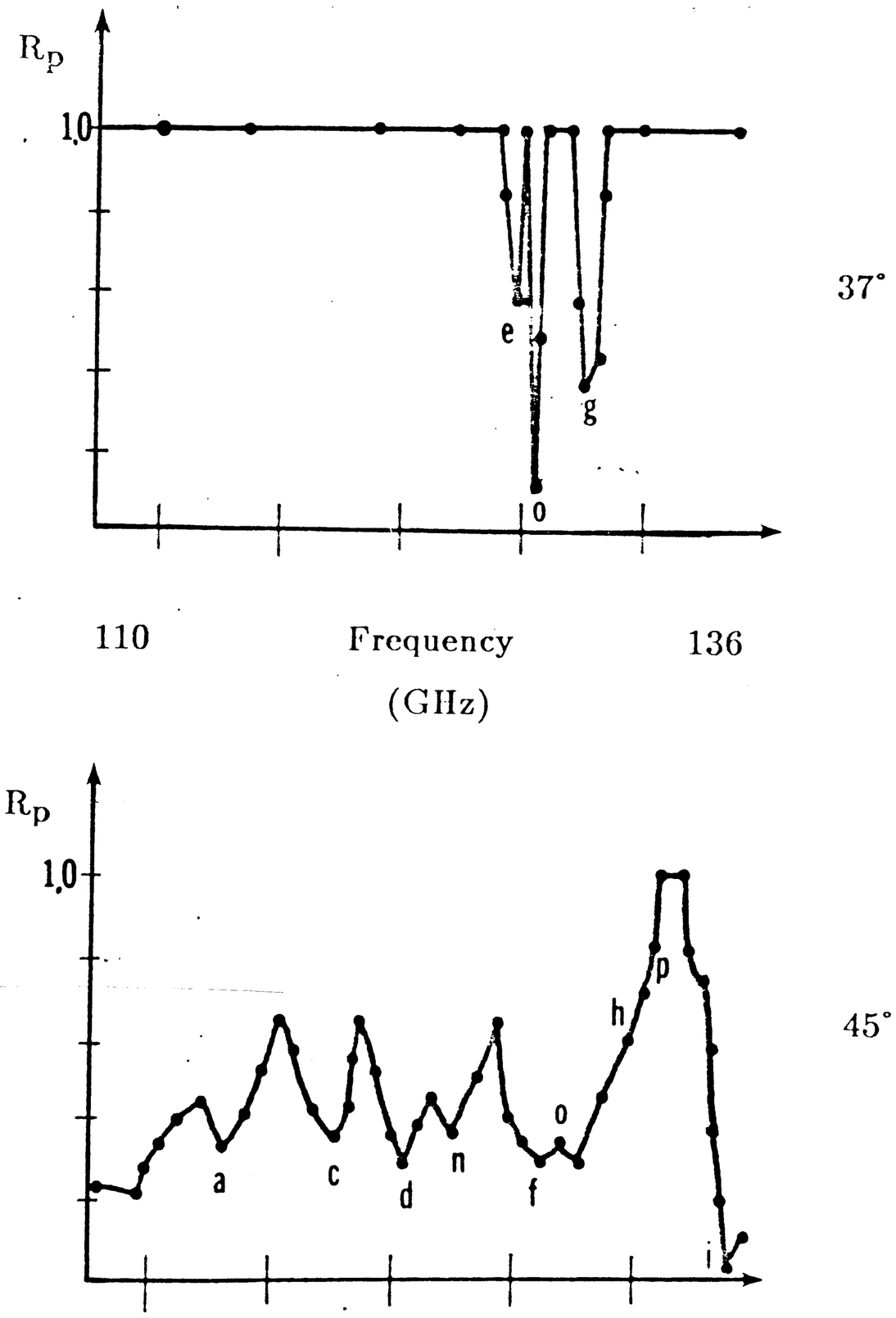

Figure 4.14 R_p vs. Frequency (θ=37°, 45°, 110- 136 GHz)

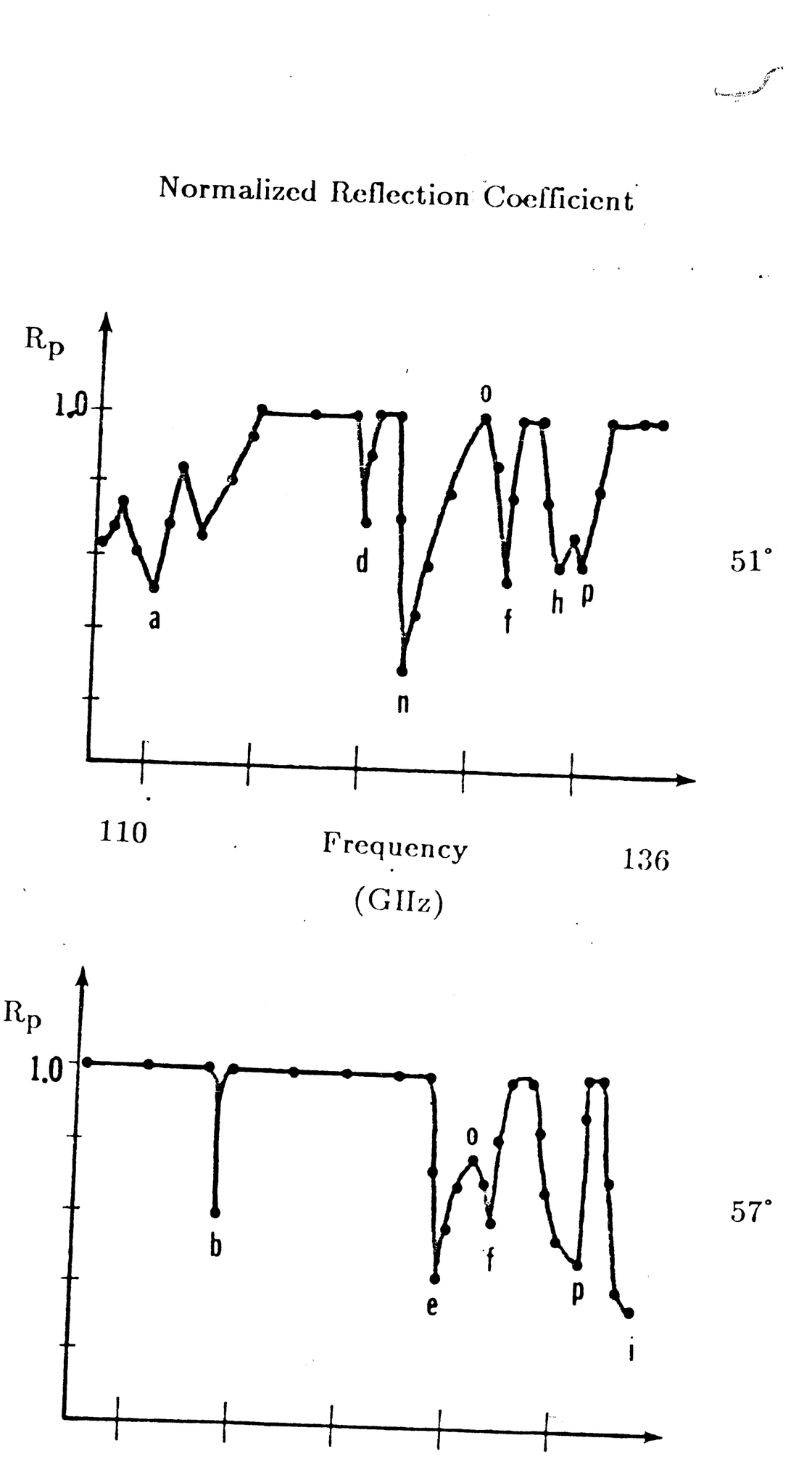

Figure 4.15 R_p vs. Frequency (θ=51°, 57°, 110- 136 GHz)

Normalized Reflection Coefficient

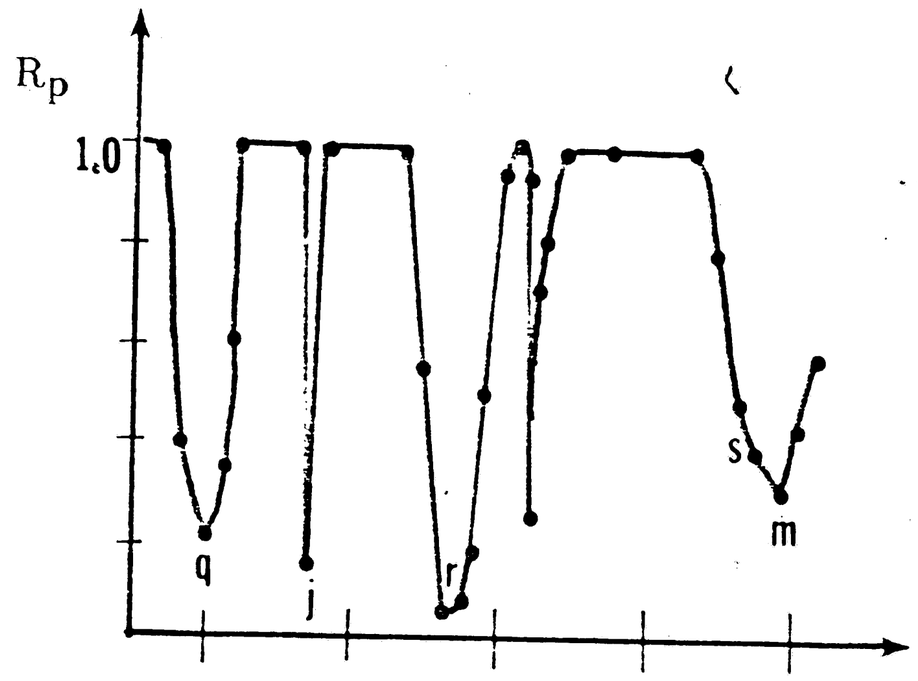

Figure 4.16 R_p vs. Frequency (θ=37°, 45°, 136- 159 GHz)

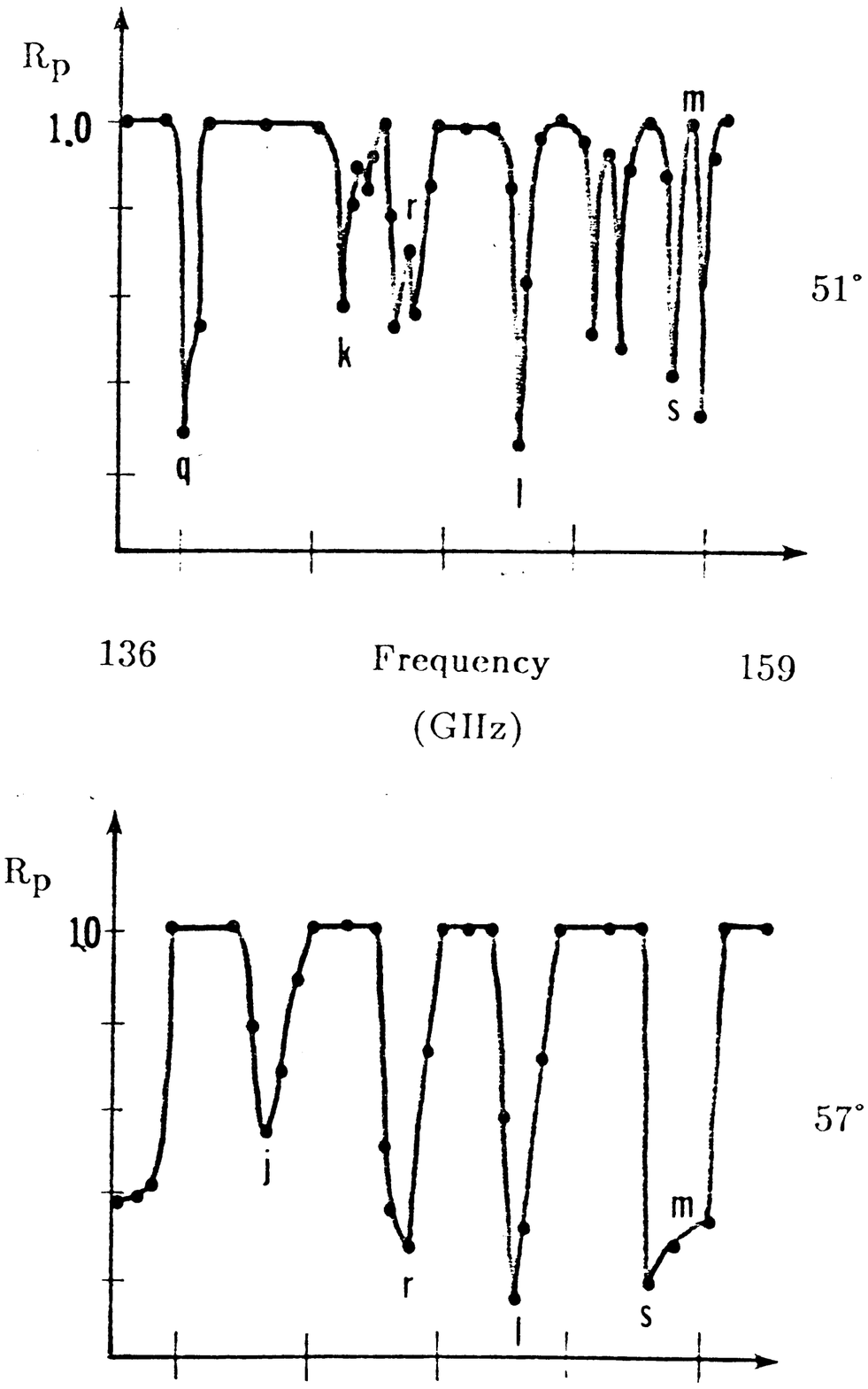

Figure 4.17 R_p vs. Frequency (θ=51°, 57°, 136- 159 GIIz)

Point	Frequency (GHz)	β (θ=37°)	β (θ=45°)	β (θ=51°)	β (rad/cm) (θ=54°)
A	115.49	23.29	27.37	30.08	32.46
B	116.38	23.47	27.58	30.31	32.71
C	120.20	24.24	28.48	31.30	33.78
D	122.93	24.79	29.13	32.01	34.55
E	127.13	25.64	30.13	33.11	35.73
F	129.23	26.06	30.62	33.66	36.32
G	130.04	26.23	30.82	33.87	36.55
H	131.49	26.52	31.16	34.24	36.96
I	135.86	27.40	32.19	35.38	38.18
J	141.80	28.60	33.60	36.93	39.85
K	145.05	29.25	34.37	37.78	40.77
L	151.89	30.63	36.00	39.56	42.69
M	157.95	31.85	37.43	41.13	44.39

Table 4.1

Experimental Data for minimum reflection points

case of a 45° angle of incidence, with the only exception occurring for point *M* which was at 51°. Consequently, table 4.1 was plotted for four bandwidths as depicted in figures 14.18 to 14.21. When the data was plotted in figure 4.22 in the form of an ω-β diagram, it showed a very close match to the theory presented in section 2.3. The 'x' points indicate dispersion points obtained using periodic couplers. It can be observed, that prism coupling provides greater accuracy when performing the experiment. The slight shift in the experimental data could mostly be accounted for by the errors contributed during the angular measurements. It could also be due to inaccurate assumptions of the refractive index of the prism (n_p=1.6). But it is not likely for a variation in the refractive index due to frequency dependence to be sufficiently large. In the periodic coupler case substantial retardation was observed. The cause of this phenomenon could be attributed to various causes. Wood's anomalies could contribute a major factor, but extensive studies and experiments would have to be carried out to prove this.

Further considerations must be given of points not mentioned in table 4.1 and R_p vs. β figures. These are *N*, *O*, *P* for the lower bandwidth of 110 to 136 GHz and *Q*, *R*, *S* for the higher band of 136 to 159 GHz. The six points mentioned show strong reduction of R_p against a frequency sweep. The lack of definite dips in the R_p vs. β plots prevent these points from being analyzed with accuracy. Interpolation will have

R_p vs. β

Normalized Reflection Coefficient

For 115.49 to 122.93 GHz

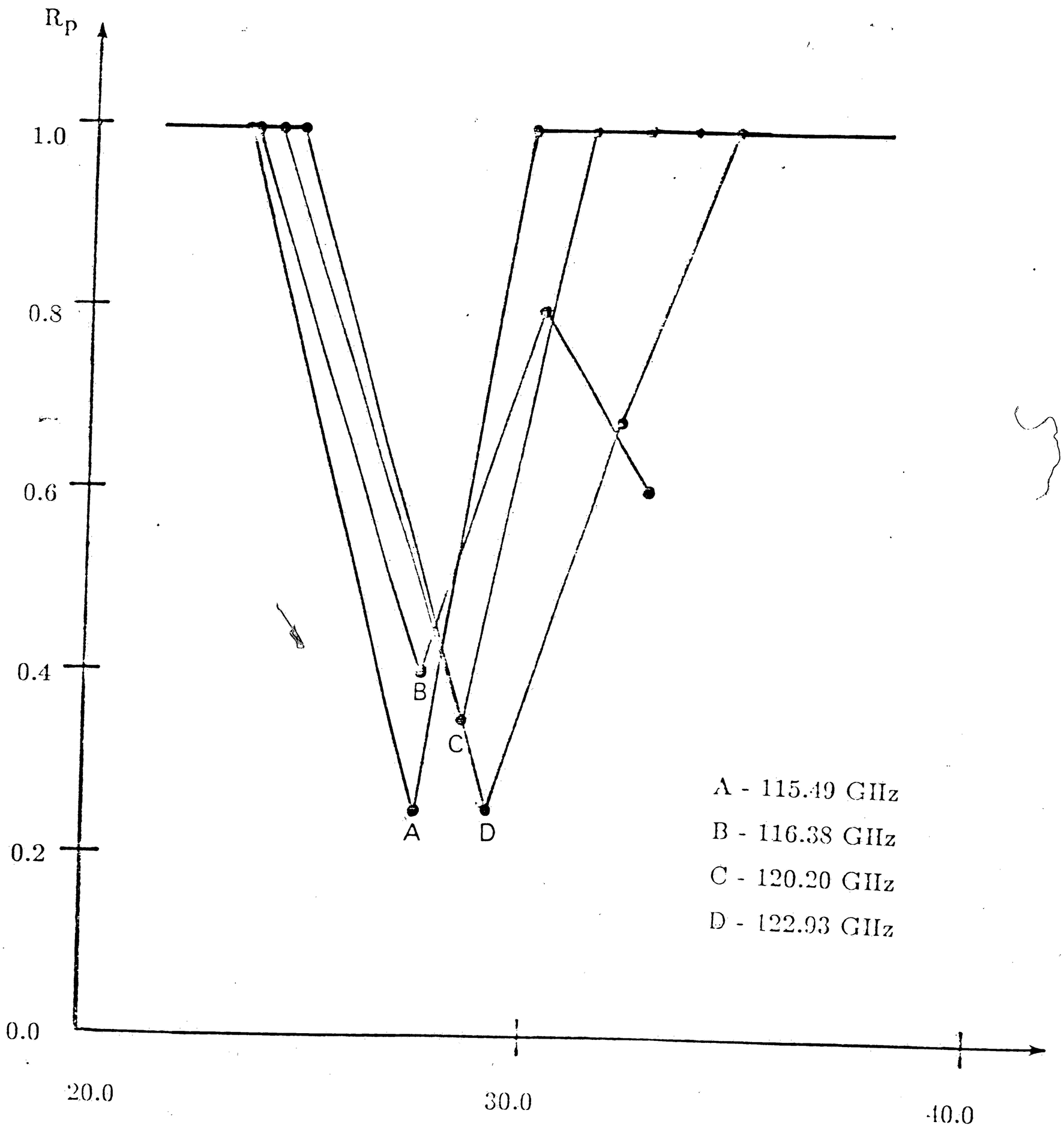

Figure 4.18 - R_p vs. β (115-123 GHz)

R_p vs. β

Normalized Reflection Coefficient

For 122.93 to 130.04 GHz

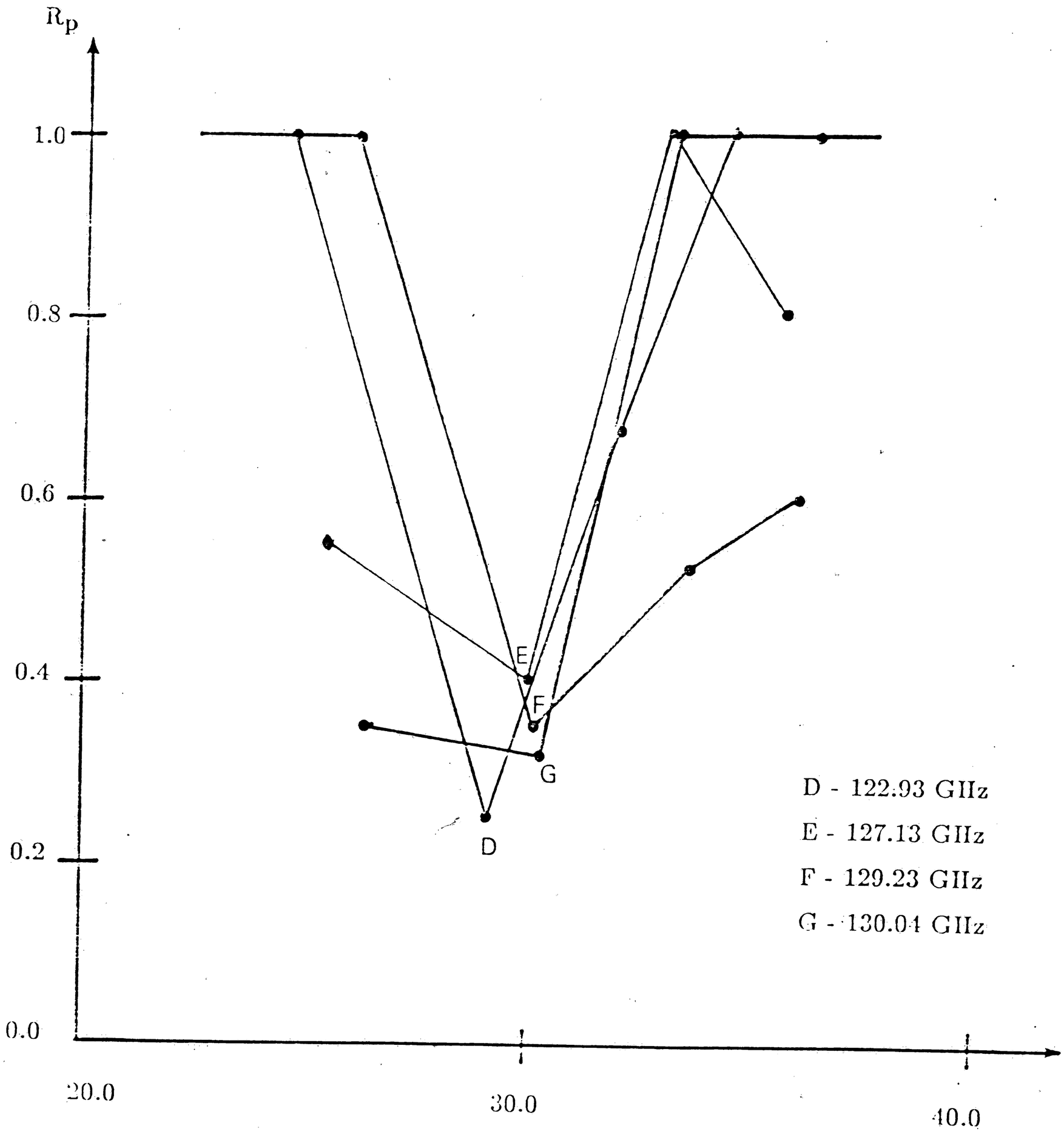

Figure 4.19 - R_p vs. β (123-130 GHz)

R_p vs. β

Normalized Reflection Coefficient

For 130.04 to 141.80 GIIz

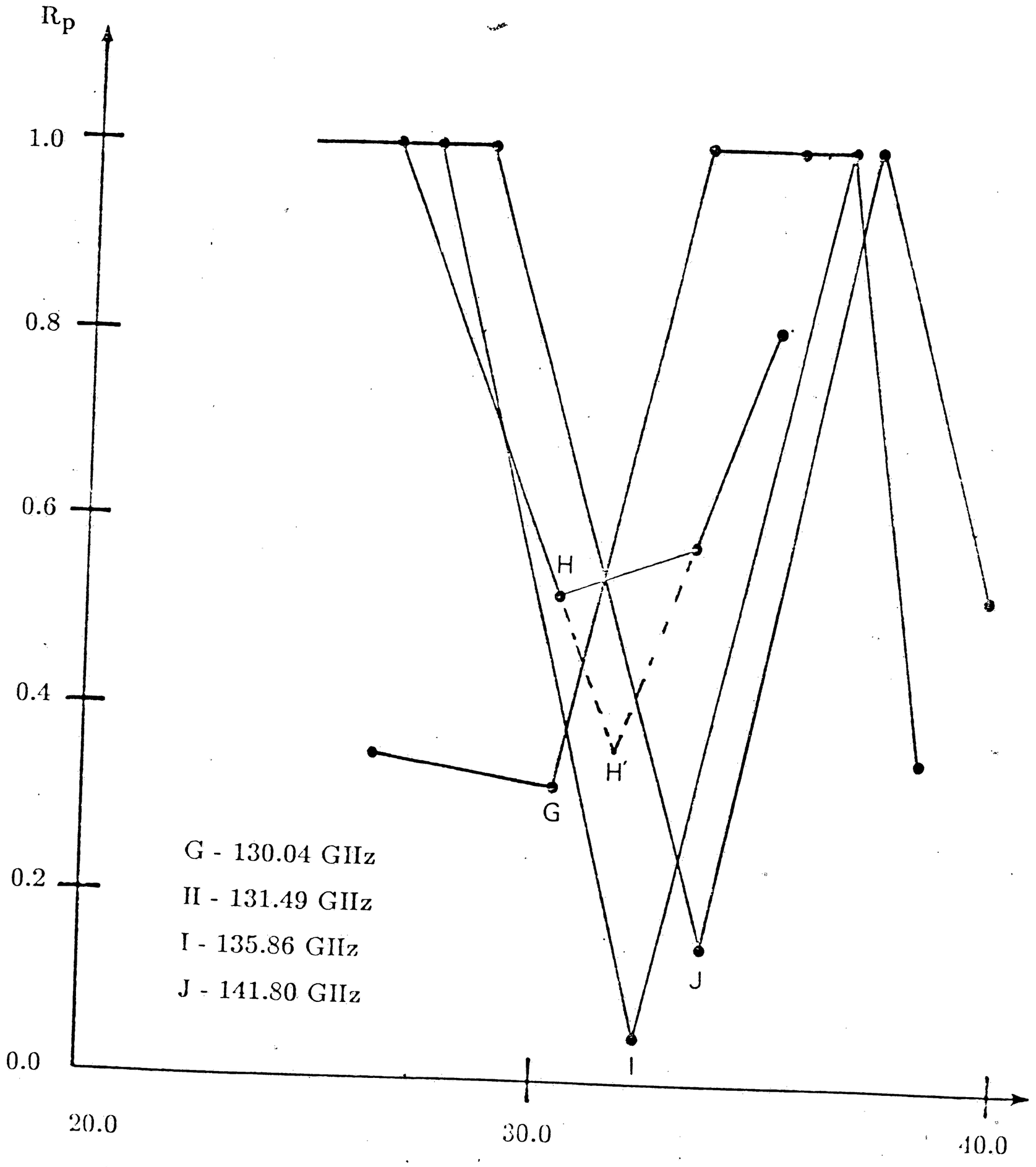

Figure 4.20 - R_p vs. β (130-142 GIIz)

R_p vs. β

Normalized Reflection Coefficient

For 141.80 to 157.95 GIIz

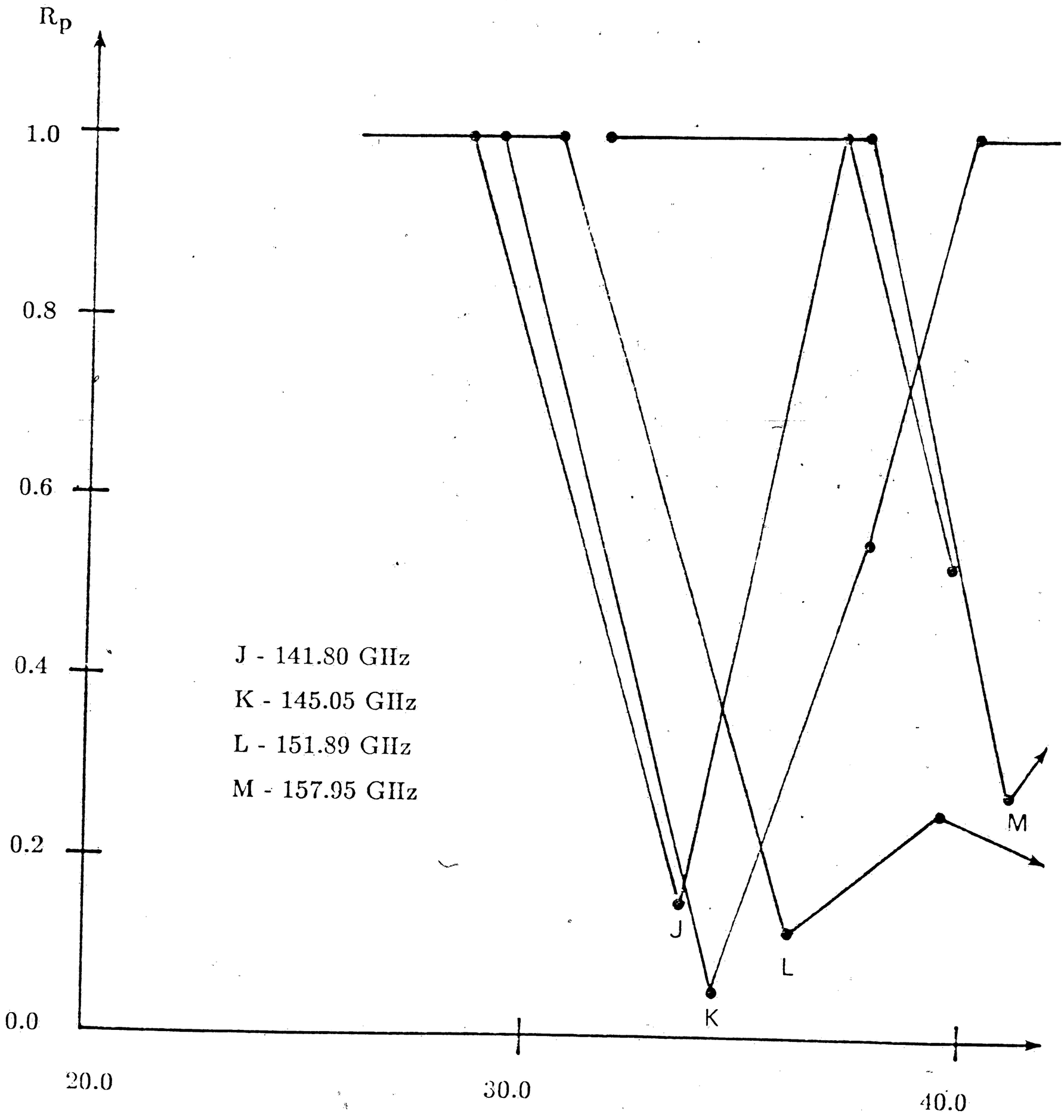

β (rad/cm)

Figure 4.21 - R_p vs. β (142-158 GHz)

ω-β Dispersion Curve

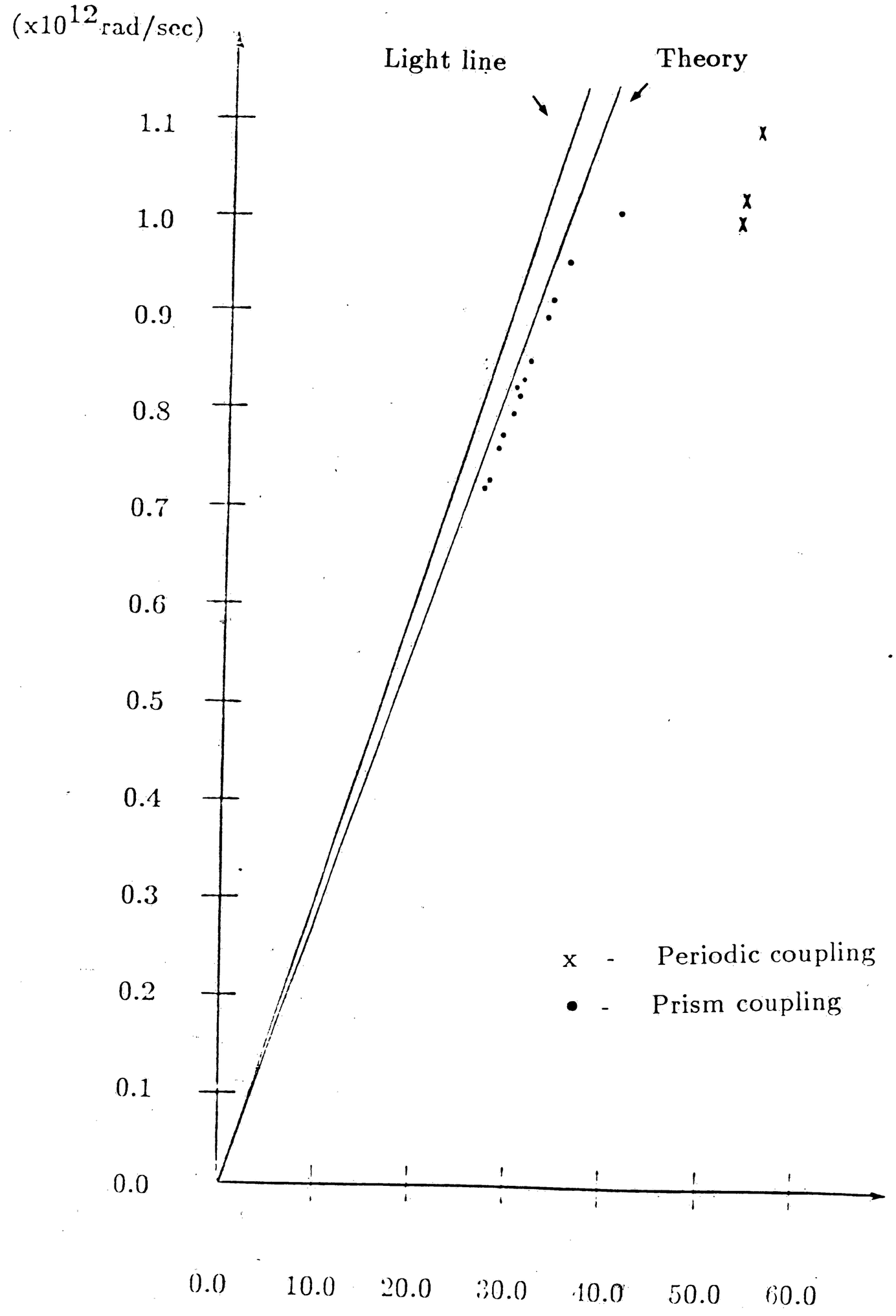

Figure 4.22 - ω-β Dispersion curve from experiment

to be used to estimate the approximate angle of incidence. In the case of point N, substantial reduction in the reflection coefficient was observed for θ=51° than θ=45°. But at θ=45° there was still about 0.7 reduction of the reflectivity, so the angle of incidence which would excite a surface plasmon would be closer to 51° but not by a large margin. The estimation for point N will be taken as θ=48°, this can be interpreted as for ω=0.7825x10^{12} rad/sec (f=124.54, point N) β=31.01 rad/cm. This value is slightly greater than the expected value, but it is within admissible margin of error. The same evaluation applies to point O with an estimated θ of 41°, ω=0.805x10^{12}rad/sec at this point with a β of 28.16 rad/cm. Point P is unique because, as the reflection angle is increased, the reflection coefficient drops. It has a high value of estimated minimum and it is the first point branching out into a second curve for the dispersion relation. With an estimated θ of 55°, point P yields to a propagation value of 38.5 rad/cm. The existence of a second mode becomes more evident when points R and S show more than one excitation angle for a single frequency. Both points R and S start at a minimum and increase to a maximum reflection around 45° and drop back to another minimum at about 55°. This point will not be included due to this uncertainty. It is probably influenced by material absorption property rather than the excitation of a surface wave. Finally, the tabulated data for the additional modal points are in table 4.2, and the final dispersion

Point	Frequency (GHz)	Minimum Angles M_1	M_2	β_1 (rad/cm)	β_2 (rad/cm)
N	124.54	48°	---	31.01	--------
O	128.10	41°	---	28.16	--------
P	132.66	55°	---	38.50	--------
Q	Discarded point				
R	147.31	39°	58°	31.10	41.86
S	157.31	40°	59°	33.88	45.19

Table 4.2

Additional data with second modal points into consideration

curve including these points , is depicted in figure 4.23.

The second set of points to the right of the dispersion curve indicate another mode contributed by the prism substrate boundary. Normally this mode is not observed in the optical regions. If no major experimental errors are exist, the only reasonable explaination for this mode is its generation by the interface adjacent to the prism. Two methods of possible verification can be suggested. First, increase the sweeper frequency to obtain a fuller dispersion curve. Second, reduce the doping density to lower the plasma frequency. The latter will also have an effect as to the range of the observable dispersion curve. If any hypothesis of the experimental errors could be made, it will be mainly due to angular measurement errors. For example, the first angle of incidence of 37° is very close to the critical angle of the prism. This error in measuring and operating in the critical angle region could have contributed to the unexpected second mode.

The final suggestion for anybody repeating this experiment would be the use of a goniometer or other accurate angular measurement device. Since our experiment, were carried out at room temperature, the next step would be to experiment under cryogenic conditions.

ω-β Dispersion Curve

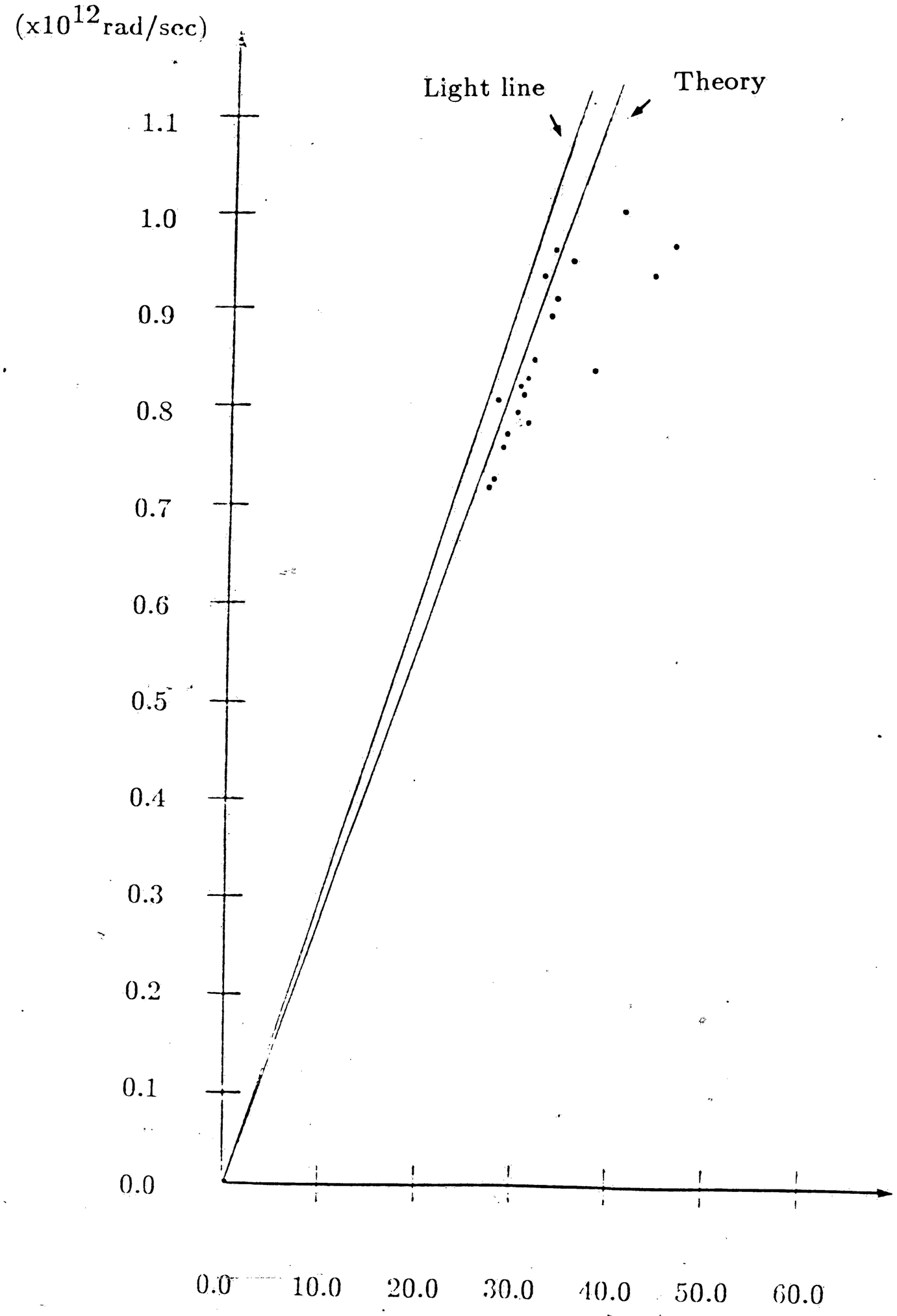

Figure 4.23 - Final ω-β Dispersion curve form experiment

V. Applications

Surface plasmons were mainly used in the optical field to analyze energy transitions and discontinuities on metal surfaces. It was also used in many studies of superconductive materials and Josephson junctions. The use of surface plasmons in the millimeter wave range as a monolithic guide to high mobility semiconductors was suggested by Nurmikko *et al.*[1], with loss calculations at cryogenic temperatures. A more recent suggestion was proposed by Bolle *et al.*[2], in theorizing nonreciprocal behavior for magneto surface plasmons on GaAs in the millimeter wave region. The achievement of surface plasmon excitation for millimeter waves brings closer a feasible means of further development of devices at this frequency range and higher. Although extensive experiments on loss and other parameters have yet to be carried out, the success in quasi-optical method of excitation and theory verification provides motivation for continued research in this field. The next logical step to follow would be on the improvement in measurement and parameter control techniques to obtain a closer match between theory and experiment. This would provide accurate control along with a reduction in losses due to increased coupling efficiency. The development of nonreciprocal devices, specifically an isolator, would allow us to test the theories. If success is encountered, other nonreciprocal devices should follow.

VI. Conclusion

Surface plasmon generation was acomplished using quasi-optical techniques. Verification was obtained through end coupling detection for the periodic coupler case, and generating R_p vs. frequency and R_p vs. β plots for the prism coupler. A better match between theory and experiment was obtained for the prism coupler. Through the experiments, the retardation effects for periodic or grating couplers were observed. The difficulty in distinguishing the correct harmonic was a problem when the profile height was tripled. Unlike the periodic coupler, the prism coupler had the advantage of generating various propagation constants for a given type of prism.

It has been shown that the non-destructive methods employed here not only is convenient, but also provides a relatively accurate detection of the surface wave dispersion characteristic. The additional mode encountered could prove to be an interesting topic for further study. In the case of optical couplers for the experiments conducted on metal surfaces, the absorption levels of the prisms encountered in the optical regions prevent such modes from existing .

Finally, the generation of surface plasmons at the frequency range of 110 to 160GHz has not been demonstrated before. The use of a highly doped n-type GaAs for such an experiment is also a first. The gap between the optical and microwave field needs to be explored for further advancement of millimeter wave devices and systems.

VII. References

[1] A. V. Nurmikko, D. M. Bolle, and S. Talisa, *Int. J. Inf.*, vol. 1, p.3 (1980)

[2] D.M. Bolle and S.Talisa, IEEE *Trans. Microwave Theory Tech.*, MTT-29, p.91(1981)

[3] N. Marschall, B. Fischer, and H. J. Queisser, *Phy. Rev. Lett.*, vol. 27, p.95 (1971)

[4] V.V. Bryksin, D. Mirlin and I.I. Reshina, *Sov. Phys. JETP Lett.*, vol.16 p.315 (1972)

[5] A. Hartstein and E. Burstein, *Solid State Comm.*, vol.14, p1223 (1974)

[6] E. D. Palik, R. Kaplan, R. W. Gammon, H. Kaplan, R. F. Wallis and J. J. Quinn, Phys. Rev., vol B13, p.2497 (1976)

[7] R.F. Wallis and C.A. Se'benne, Handbook on Semiconductors, M. Balkanski Ed., vol 2, Ch.3, (1980)

[8] A. Otto, Optical properties of Solids-New Developments, B. Seraphin Ed., vol.2, Ch.12, (1975)

[9] R. F. Harrington, Time-harmonic electromagnetic fields, Ch.4, (1961)

[10] D. L. Lee, Electromagnetic principles of integrated optics, Ch.4, (1986)

[11] B. Fischer and N. Marschall, *Proceedings of the 10th Internatinal Conference on the Physics of Semiconductors,* S.P. Keller, J.C. Hensel, and F. Stern, eds., p. 845 (1970)

[12] B. Laks, D. L. Mills, and A. A. Maradudin, *Phys. Rev-B,* vol B23, p. 4965 (1981)

[13] J. Hagglund and F. Sellberg, *J. Opt. Soc. Am.*, vol. 56, p. 1031 (1966)

[14] T. Tamir and H. J. Berton, *J. Opt. Soc. Am.*, vol. 61, p. 1397 (1971)

[15] T. Tamir, Topics in Applied Physics - Integrated Optics" vol. 7, p. 113 (1979)

[16] C.A. Ward, R.J. Bell, R.W. Alexander and G.S. Kovener, *Appl. Opt.* vol.13, p.2378 (1979)

[17] R. Ulrich, J. Opt. Soc. Am., Vol.60, p. 1337 (1970)

[18] J. H. Harris, R. Shubert, IEEE Trans. Microwave Theory Tech., Vol. MTT-19, p. 269 (1971)

[19] A. Otto, Z. Physik, Vol. 181, p.232 (1965)

[20] E. Kretschmann, Z. Physik Vol. 241, p. 313 (1971)

[21] S.M. Sze, Physics of Semiconductor Devices, p.33 (1981)

VIII. Vita

Dong-Hyun Hwang was born in Seoul, Korea on November 6th 1963. He is the only child of Mr. Young-Jae Hwang and Mrs. Jung-Ae Choe. Mr. Hwang graduated with honors from Tenafly High School in Tenafly, New Jersey on June of 1982. He attended Lehigh University as an undergraduate between August 1982 to January 1986, where he graduated with high honors with a Bachelor of Science degree in Electrical Engineering. He continued his graduate studies at Lehigh University from January 1986 to June of 1988. As a graduate student, he worked as a teaching and research assistant for the Department of Computer Science and Electrical Engineering.